Effects of climate change in the European croplands and grasslands: productivity, GHG balance and soil carbon storage

Marco Carozzi[1,a], Raphaël Martin[2], Katja Klumpp[2], Raia Silvia Massad[1]

[1] Université Paris-Saclay, INRAE, AgroParisTech, UMR ECOSYS, 78850, Thiverval-Grignon, France
[2] INRAE, UREP Unité de Recherche sur l'Ecosystème Prairial, F-63100 Clermont-Ferrand, France
[a] now at: Université Paris-Saclay, INRAE, AgroParisTech, UMR SADAPT, 78850, Thiverval-Grignon, France

Correspondence to: Marco Carozzi (marco.carozzi@inrae.fr)

Abstract.

The knowledge of the effects of climate change on agro-ecosystems is fundamental to identify local actions aimed to maintain productivity and reduce environmental issues. This study investigates the effects of climate perturbation on the European crop and grassland production systems, combining the finding from two biogeochemical models. Accurate and high-resolution management and pedoclimatic data has been employed. Results has been verified for the period 1978-2004 (historical period) and projected until 2099 with two divergent intensities IPPC's climate projections, RCP4.5 and RCP8. We provided a detailed overview on productivity and the impacts on management (sowing dates, water demand, nitrogen use efficiency). Biogenic GHG budgets (N_2O, CH_4, CO_2) were calculated, including an assessment of their sensitivity to the leading drivers, and the compilation of a net carbon budget over production systems. Results confirmed that a significant reduction of productivity is expected during 2050-2099, caused by the shortening of the length of the plant growing cycle associated to the rising temperatures. This effect was more pronounced for the more pessimistic climate scenario (-13 % for croplands and -7.7 % for grasslands) and for Mediterranean regions, confirming a regionally distributed impact of climate change. Non-CO_2 GHG emissions were triggered by rising air temperatures and increased exponentially over the century, being often higher than the CO_2 accumulation of the explored agro-ecosystems, which acted as potential C sinks. Emission factor for N_2O was 1.82 ± 0.07 % during the historical period, rising up to 2.05 ± 0.11 % for both climate projections. The biomass removal (crop yield, residues exports, mowing and animal intake) converted croplands and grasslands into net C sources (236 ± 107 Tg CO_2eq y^{-1} in the historical period), increasing of more than 20 % during the climate projections. Nonetheless, crop residues demonstrate to be an effective management strategy to overturn the C balance. Although with a marked latitudinal gradient, water demand will double over the next few decades in the European croplands, whereas the benefit in terms of yield will not contribute substantially to balance the C losses due to climate perturbation.

1   Introduction

Agriculture is facing a major challenge to meet growing food demand while limiting soil degradation, air and water pollution, and adapting to climate change impacts (Chaudhary et al., 2018; Olesen, 2017). Agricultural sector is the main source of non-

CO$_2$ anthropogenic greenhouse gases (GHG) and is responsible for 78.6 % of nitrous oxide (N$_2$O) and 39.1 % of methane (CH$_4$) emissions worldwide (IPCC, 2018). Agricultural practice, which directly affect soil, plant and atmosphere represent a

35   strategic lever to counteract climate change by mitigating GHG emission and fostering soil C storage (Chabby et al., 2017, Smith et al., 2008) achieving long-term (*i.e.* 2100) climate objectives (Fuss et al., 2016; Minasny et al., 2017; Smith et al., 2013).

Evaluating the impacts of climate on agricultural productions at local, regional and global scales is still a challenge nowadays (Fitton et al., 2019; Olesen and Bindi, 2002). The main source of uncertainty come from the representation of agroecosystems

40   in models' framework, or from the approaches used to upscale local experiments to regional scales (Ewert et al., 2011; Tubiello et al., 2007). Notwithstanding that, is commonly recognised that a decrease in crop yields is expected towards the mid and the end of the century, with reductions extending to more than 10 % in some region of the world (Challinor et al., 2014). Decline in productivity is likely to be combined with an increase of the interannual yield variability due to climate extremes (Dono et al., 2016), and with a strong latitudinal gradient (Rosenzweig et al., 2013). In the northern hemisphere, which will benefit from

45   the lengthening of the growing season, milder temperatures and wet conditions in the next decades, crop and grassland productions are expected to rise (Yang et al., 2015). Conversely, lower latitudes are going to face a rise of drought frequencies with a decline of winter rainfall, accompanied by a potential decline in productivity (Stagge et al., 2017). This geographical gap would lead to an intensification of farming systems in northern regions, as north Europe, to an extensification in the southern regions, as the Mediterranean basin (Olesen and Bindi, 2012).

50   In line with the commitment to the Paris Agreement and the European Green Deal, EU set the objective to cut net GHG emissions by at least 55 % by 2030, compared to 1990 levels. In addition, EU aims to became climate neutral by 2050 (EC, 2020). This ambitious target contrasts with agricultural emission which stagnated or even increased in the past few years (EEA, 2020). Reducing emission imply the use of management options in crop and grassland systems aimed to increase the efficiency of fertilisers and feeding strategies, manage crop residues, tillage operations, irrigation and drainage, and increasing cropping

55   diversification (Aguilera et al., 2013; Conant et al., 2017; Cowan et al, 2016; De Antoni Migliorati et al., 2015; Li et al., 2016; Smith et al., 2008; Smith, 2016, Voglmeier et al., 2019). While there is a consistent amount of experimental data regarding management options, a robust quantification of the effects of climate change on the actual crop and grassland production systems at regional scale are still scarce. Concurrently, the need to develop and implement higher tier methodologies to be applied at fine spatial scales is growing nowadays (Smith, 2012).

60   Dynamic simulation models are suitable tools to evaluate the multifaceted effects of climate change across agricultural production systems as croplands and grasslands (Ehrhardt et al., 2018; Brilli et al., 2017; Sándor et al., 2018). Models are able to isolate the contribution of single or combined factors, trace the evolution of the system components and observe the aptitude of the agricultural strategies to mitigation impacts. More recently, process-based models conceived for site scale representation were applied at the regional scales to *e.g.* calculate national GHG inventories (Smith, 2013) or build statistical models (Del

65   Grosso et al., 2009; Haas et al., 2013). Major challenges to perform spatial assessment are represented by the availability of input data (Lugato et al., 2014; 2017), the representativeness of the model to change of spatial scale (Hoffmann et al., 2016)

and bias introduced in the aggregation or disaggregation of input data in representative homogeneous spatial areas (Constantin et al., 2019). Furthermore, simulating agricultural productions with climatic projections, introduce a further degree of uncertainty, which can be reduced by performing a sound assessment over historical data as proposed in this study (Rosenzweig 70 et al., 2013).

This research aims to investigate, by means of simulation modelling, the contribution and the impacts of climate change in the European cropland and grassland production systems towards year 2100. The analysis focuses on plant productivity and biogenic GHG (N_2O, CH_4, CO_2) balance, outlining a detailed carbon budget with two climatic scenarios, one intermediate and one pessimistic. This study represents the baseline to support and identify future actions targeted to maintain productivity and 75 reduce environmental impacts.

2   Material and Methods:

The study was realised by using two agro-ecosystem models, CERES-EGC for cropping systems and PaSim for grassland-livestock systems. Models were run on a spatial resolution of 0.25°, which is equivalent to an aggregation of the output to a squared cell of 27.78 km side. Each cell has its specific soil properties, agricultural management and daily climatic data. The 80 0.25° grid was identified to attain an adequate representativeness of the spatial variability of the inputs, a representativeness of the local effects at European scale, and limit computational burdens (Hoffmann et al., 2016; Constantin et al, 2019).

2.1   Models

CERES-EGC (Crop-Environment REsources Synthesis – Environement et Grandes Cultures) model was used to simulate crop rotations in EUROPE. CERES-EGC is a process-based biogeochemical model in the soil-plant-atmosphere domain 85 adapted from CERES (Jones and Kiniry, 1986). The model is designed to simulate C and N dynamics, the transfer of heat and the water exchanges from soil and plant with a daily time step, at the field scale (Gabrielle et al., 2005). Inputs require meteorological and management data as forcing variables and soil and crop data as factors. Meteorological data are constituted by daily minimum and maximum temperature, precipitation, global solar radiation and wind speed. Management includes tillage, irrigation, fertilisation, information of sowing and incorporation on crop residues. Soil is divided in sublayers with 90 specific depth, and physical and chemical characteristics. Simulated crop species include maize (grain and fodder), soft wheat, durum wheat, rye, oat, barley, rapeseed, sorghum, sunflower, pea, sugar beet and soybean, with the possibility to select specific cultivars.

Soil C and N dynamics in the ploughed layer are simulated by means of the NCSOIL model (Molina et al., 1983; Nicolardot et al., 1994), which is a nested module in CERES-EGC. NCSOIL compute nitrification, immobilisation and mineralisation of 95 N, the decomposition of soil organic matter (SOM) after incorporation of crop residues and SOM formation. The module works with a series of specific pools, three pools for crop residues (easily fermentable carbohydrates, cellulose and lignin) and four endogenous pools (zymogenous and microbial biomass, active and passive humus), where CO_2 is released from the

decomposition of each pool. N uptake by plants is calculated through a specific supply/demand scheme depending on mineral nitrogen availability and root length density. CERES-EGC includes the model NOE (Hénault et al., 2005) for simulating N_2O

100 emissions from denitrification and nitrification processes in the topsoil (0-20 cm depth). Denitrification and nitrification are computed from a soil-specific potential rate limited by unitless factors related to soil water content, soil temperature and substrate content (nitrates, NO_3, and ammonium, NH_4, for denitrification and nitrification, respectively). Plant growth is simulated according to the crop specific genetic potential and the photosynthetically active solar radiation absorbed by the canopy. Potential dry matter production is constrained by air temperatures, soil water availability and N deficit.

105 **PaSim** (Pasture Simulation model) is a biogeochemical process-based model able to simulate C, N and water dynamics in the soil-plant-animal-atmosphere grassland system (Riedo et al., 1998; Calanca et al., 2007). Five interacting sub-models of soil biology and physics, microclimate, vegetation and grazing herbivores constitute the model structure. The model runs on daily (or hourly) time step and inputs require soil property data, management and meteorological characteristics (global solar radiation, minimum and maximum air temperature, relative humidity, wind speed, precipitation and atmospheric CO_2

110 concentration). The soil is described in six sublayers allowing to parametrise different soil depths with site-specific soil physical and chemical characteristics. Management includes grazing, mowing, N fertilisation. Grazing is considered as a dairy or suckling system managed by grazing periods with specific stocking density and live weight. Indoor periods are not simulated. Vegetation cover is considered as a homogeneous cover with a fixed legume fraction. The vegetation cover comprises root system and three shoot compartments (laminae, sheaths and stems, ears) divided into age classes. Soil C

115 dynamics (based on CENTURY model; Parton et al., 1994) are computed in five pools, a structural and a metabolic pool for fresh organic carbon (plant residues), and an active, a slow and a passive pool for the microbial processed organic carbon. Photosynthetic C is allocated in plant (root and shoot) and can be lost as CO_2 by ecosystem respiration and as CH_4 through enteric fermentation.

Soil N inputs are represented by atmospheric N deposition, symbiotic N_2 fixation, mineral or organic fertilisation, animal

120 faeces and urine. These inputs, together with the nitrogen mineralised from the organic carbon pools, constitute the mineral N pool. N availability for plants is reduced by losses via processes of immobilization, NO_3 leaching, NH_3 volatilization, nitrification and denitrification processes. N_2O emission from nitrification and denitrification depends on substrate availability (NO_3 or NH_4). These emissions are modulated by factors controlling the effects of soil temperature and water content. Furthermore, the release of N_2O produced into the soil toward the atmosphere is calculated with a resistance model in the

125 rooting zone and plant canopy (Schmid et al., 2001).

CERES-EGC and PaSim were selected as the most suitable models for a spatialized assessment since they have been calibrated and evaluated in different European conditions (Brilli et al., 2017; Ehrhardt et al., 2018; Sandor et al., 2018; Ma et al 2015) and because they are able to simulate gaseous emissions. Both models can globally simulate a number of crops and rotations, mown or grazed grasslands, and the effects of management practices on plant-soil- atmosphere interactions. Besides, both

130 models are able to simulate the carbon budget at the field scale, through the C assimilated from the photosynthesis, C emitted into the atmosphere from autotrophic and heterotrophic respirations, C recycled into the system (dung, plant residues) or

introduced from external sources (fertilisers, soil improvers), and the C exported from the system by production activity. CO_2 fertilisation was not simulated for croplands (see S.4 in the supplementary material). Furthermore, the simulation models used in this study do not represent potential impacts of air pollution, pest and disease effects.

135 ## 2.2   Input data set

2.2.1   Climate data

Historical and climate projections data were used in this study to analyse the likely effect on GHG, productions and soil C stocks in European production systems. We selected two of the four climate scenarios, or "Representative Concentration Pathways" (RCPs) adopted by the IPCC for the fifth Assessment Report (AR5) (IPCC, 2013), an intermediate scenario,
140 RCP4.5, and a pessimistic one, RCP8.5.

Climate data were provided by the Earth System model HadGEM2-ES (Collins et al., 2011) and were downscaled to a horizontal grid with 0.5° side resolution in the framework of the Inter-Sectoral Impact Model Intercomparison Project (ISI-MIP; Warszawski et al., 2014). Since the spatial resolution of the climatic data is larger than the size selected for the simulation units (0.25°), 4 adjacent simulation units were subjected to the same meteorological data. Data were not downscaled to
145 maintain data accuracy as much as possible. Data has been shaped for the European surface (29.0° to 71.5° Latitude and -24.0° to 45.5° Longitude). HadGEM2-ES model provided daily values of minimum and maximum air temperature, total precipitation, air specific humidity, shortwave radiation and near surface wind speed, for the period 1951-2099. Based on these data, input variables for each model were assigned. The simulation protocol consists of a historical dataset, from 1978 to 2004, constituted in accordance with HadGEM2-ES model using the historical record of climate forcing factors (Jones et al., 2011),
150 and two climate projections RCP4.5 and RCP8.5, from 2005 to 2099.

2.2.2   Soil data

Soil data were obtained from the European Soil Database (ESDB; Hiederer, 2013). The ESDB is composed by 1 km × 1 km raster files containing topsoil (0 to 30 cm) and subsoil (30 cm to maximum soil depth) data of clay, silt, sand, gravel, and soil organic carbon (SOC) content, bulk density and maximum root depth. Soil pH for the topsoil was derived at the same spatial
155 detail from the ESDB dataset provided by Reuter et al. (2008). To define soil characteristics for each spatial simulation unit of 0.25° side, the most frequent soil was selected, accordingly with their characteristics. Model-specific soil input parameters were calculated on the base of the elementary characteristics (see supplementary material S.1 for details). For both models, a fixed number of six soil layers was established with a thickness defined as a function of the maximum soil depth. Organic soils with SOC content over 30 % were excluded from the simulations (3.4 % of the total simulation units).

160 **2.2.3   Crop data**

Crop species and N fertilisation amount for European Union on the 1 km × 1 km grid were provided in the framework of the GHG-Europe project (EU FP7; Wattenbach et al., 2015). These data are based on the statistical crop distribution of Eurostat database (European Statistical Office, 2019a) at regional scale (NUTS2 regions), and the simulation of the CAPRI model (Common Agricultural Policy Regionalized Impact; Britz and Witzke, 2008; see Leip et al., 2008). Nitrogen fertilisation
165   amount and the repartition between mineral and organic forms were also provided at NUTS 2 scale.

Crop successions were available for the period 1976 to 2010. We only considered the crop successions from the time interval 1978 to 2010 since the crop species used in the two discarded years (1976-1977) were never reused over the time series, and represented less than 1 % of the crop successions (*i.e.*, summer cereal mixes without triticale, other cereals including triticale, winter barley, flax, hemp and set aside). The two most frequent crop successions were selected as a reference for each
170   simulation unit. In fact, they cover on average up to 93 % of the total agricultural area of the simulation units (median over all the simulation units with two rotations equal to 100 %). Based on this aggregation, the simulated crops were: summer/spring soft wheat, winter soft wheat, durum wheat, summer/spring barley, grain maize, fodder maize, rapeseed, sunflower, s, pulses, potato and sugar beet. Crop rotations included also winter rye, rice and potato, which were not explicitly parameterised in CERES-EGC model, and were respectively substituted with soft wheat for rye and rice (the latter in the end was not represented
175   in the rotations) and with sugar beet for potato. To define the crop species in the period 1951 to 2099, primary and secondary successions were replicated for all the years preceding and succeeding the time interval of available data (1978-2010). Furthermore, most adapted and calibrated crop varieties were designated in function of the latitude, based on previous work and modellers' experience.

Sowing dates were defined for each crop specie, for each simulation unit and per year, based on a crop-specific time window,
180   as well as a minimum and a maximum threshold temperature. Crop-specific windows were extracted from the assessments of USDA (1994) and Sacks (2010), selecting the minimum and the maximum typical sowing span over Europe, whereas threshold temperatures were extracted from Steduto et al. (2012). Given their width, time windows were not changed over time. The sowing date was defined as the earliest within the time window, when minimum and maximum temperatures were respectively higher and lower than the thresholds. An additional constraint (no precipitation for three days in a row) was applied to consider
185   farmers practice concerning access to the field. If a suitable sowing date was not identified, a fixed date was imposed in the middle of the time window. Crop database considers a unique crop harvested per year. Residue were managed based on crop type, exporting all the cereals straws (80 % harvested straw of cereals including fodder maize), and leaving the residues of all the other crop types in the field, including grain maize (Eurostat, 2013). Typical sowing crop densities were imposed based on Steduto et al. (2012). Fertilisation amounts (kg N ha^{-1} year^{-1}) were defined as the average amounts designed for each of the
190   crops in the most frequent succession in the simulation unit. Splitting and fertilisation dates were established based on crop type and the sowing date, total nitrogen amount and mineral to organic repartition (see supplementary material S.2 for details).

Irrigation was automatically supplied to the simulation unit which are defined as irrigable in the EU for the year 2016; "irrigable" is considered as the area equipped for irrigation greater than 5 % of the utilised agricultural area (Eurostat 2019b). This share was 36 % of the EU and is mainly in the Mediterranean area, southern France and north-west of France, the

195 Netherland and some regions in Denmark, Germany and the UK. The amount of water was distributed automatically at the rate of 10 mm d^{-1} when the soil available water content was below 90 %. This means that non-irrigated crops had access to irrigation water. Even if in the coming decades the global irrigated area is not expected to grow further due to water scarcity and limited land (Turral et al., 2011), to account for a possible increase of the irrigable share toward 2100, a management scenario to observe the maximum potential irrigation water demand for today's crops grown in Europe was simulated and

200 discussed. This management is evaluated over the century by the two scenarios i_RCP4.5 and i_RCP8.5.

2.2.4 Grassland and livestock data

Grasslands data considered permanent grassland and rainfed temporary grassland. Nitrogen fertiliser application for European grasslands in a 0.25° side resolution grid was estimated on the base of regional and national statistics (Eurostat) and CAPRI model (Leip et al., 2008). Data were generated combining fertilization managements and nitrogen doses, together with number

205 of mowing events, animal loads, amount of mineral fertilizers and / or organics, and the fraction of leguminous. Mowing dates were defined from temperature using thermal sums (500 °C-days from the first of January) on a base of 5 °C. No cutting was performed before such thermal sums was not obtained. Fertilisation events occurred three days after mowing. Grazing started 30 days after the first mowing event and ended either at the end of the year or at the first freezing period of five consecutive days. Livestock were represented in the model only by cattle. Livestock densities (LSU ha^{-1}) were obtained from 0.05° side

210 regional statistics (Wint and Robinson, 2007) multiplying the total number of animals per surface unit to 0.8, 0.1, and 0.1 for cattle, sheep and goats, respectively. Finally, LSU density distribution was aggregated to the 0.25° side grid. As for cutting and fertilization, if no thermal sums were reached, then no events were performed. Biomass production is considered as the sum of the grazer intake and the cut biomass. For each grid cell, livestock is only fed by grass (*i.e.* no external feed is considered). If the amount of daily aboveground biomass is not sufficient to grazing animals, animals are moved from the

215 pasture. In this study we simulate livestock as they contribute to N cycling and since are an important source of nitrogen in grassland, although we do not discuss here their productions.

2.2.5 Models spin-up and computation

The models were set to equilibrium through a spin-up run using the period from year 1951 to 1977. This period was necessary to reach equilibrium of the soil C and N pools with the specific land use of the simulation unit and obtain reasonably realistic

220 outputs. For croplands we assumed that the cultivated area during the spin-up was likely to have been continuously cultivated with the same crop successions. For grasslands, transformation rules were applied to move from past towards current management practices, *i.e.* from 1901-1950, a low intensification management level with no mineral fertilization and cut at 900°C-days were applied. From 1951 to 2010, there was a gradual management intensification up to achieving the target levels

(linear increase of quantities, progressive earlier shift of cutting date). In this period, mineral nitrogen fertilization was applied,
225 starting with a low level in 1951. Finally, from 2010 to 2100, constant management according to the protocol come into effect. Models were initialised with the chemical and physical soil parameters derived from the ESDB relative to the year 2013. A total of 86724 run divided in two land uses (8861 for arable, with two climate scenarios, two crop rotations and two irrigation scenarios; 7918 unit for grasslands, with two climate scenarios) were simulated in a dedicated server.

2.3 Greenhouse gas exchange and balance

230 For assessing the net greenhouse gas exchange (NGHGE) of the investigated ecosystems, the contribution of the biogenic GHG (CO_2, N_2O, CH_4) is combined and normalised to grams CO_2-equivalents by using the relative global warming potential (γ_gas) at the 100-year time horizon (298 for N_2O, 25 for CH_4 and 1 for CO_2; IPCC, 2018), following the approach presented by Soussana et al. (2007):

$$NGHGE = NEP + \gamma_{N_2O}F_{N_2O} + \gamma_{CH_4}F_{CH_4}$$

235 The net ecosystem production (NEP) is the amount of organic C available for net ecosystem C storage, export or loss in an ecosystem, in terms of CO_2. NEP represents the difference between the gross primary production, or photosynthesis, and the ecosystem respiration, which is the sum of the autotrophic and heterotrophic respirations (HR); ruminant respiration from grasslands ecosystems is not accounted in the HR term. Conventionally, a negative value of NEP stating an uptake of CO_2 by the system, whereas a positive value is a release in atmosphere.

240 The annual net greenhouse gas balance (NGB) is calculated on the base of Ammann et al. (2020) by including the export of C by harvested biomass (crop yield, mowing and animal intake), the export of crop residues and the import of C by manure (organic fertilizers and the excreta from grazers):

$$NGB = NGHGE + F_{C-harvest} + F_{C-residues} - F_{C-manure}$$

As livestock were not grazing all year, their contribution to the carbon balance is represented by the intake of biomass, enteric
245 fermentation (CH_4) and C in excreta. Carbon emissions from farm operations (*i.e.* tractor emissions), erosion and leaching processes, fire or off-farm emissions (*i.e.* fertiliser manufacture, barns) are not included in the C budget, as well the effects of volatile organic compounds and CH_4 emissions from manure and from soil are considered as negligible. Moreover, the C exported from animal production (body mass increase and milk production) is neglected from NGB calculation (*e.g.* Chang et al., 2015).

3 Results:

3.1 Cropland and grassland productions

3.1.1 Model validation

Simulated crop yields during the historical period ranged between 1.4 and 44.8 t ha^{-1} (as standard humidity) and were in good agreement with EU statistics reported in the Eurostat database (Eurostat, 2020) for the time span 1978-2004 (Fig. 1a; the time span considered represents the original crop rotation data and complies with the beginning of the climate scenarios). Root Mean Squared Error (RMSE) was equal to 2.24 t DM ha^{-1}, Mean Absolute Error (MAE) to 1.35 t DM ha^{-1} and the modelling efficiency (Nash and Sutcliff, E) scored 0.97. Simulations with CERES-EGC overestimated the yields for grain maize, wheat, rye, soybean and sunflower, whereas potato, pulses, rapeseed, barley and sugar beet were slightly underestimated. The relative RMSE (RRMSE) for each crop, individually, ranged from 12.8 to 38.6 %. Furthermore, reducing the simulation period to 1994-2004 to limit the effect of the crop annual genetic gain on measured data, the statistics above described were not modified. Representative data for grassland productions are still scarce at EU-level.
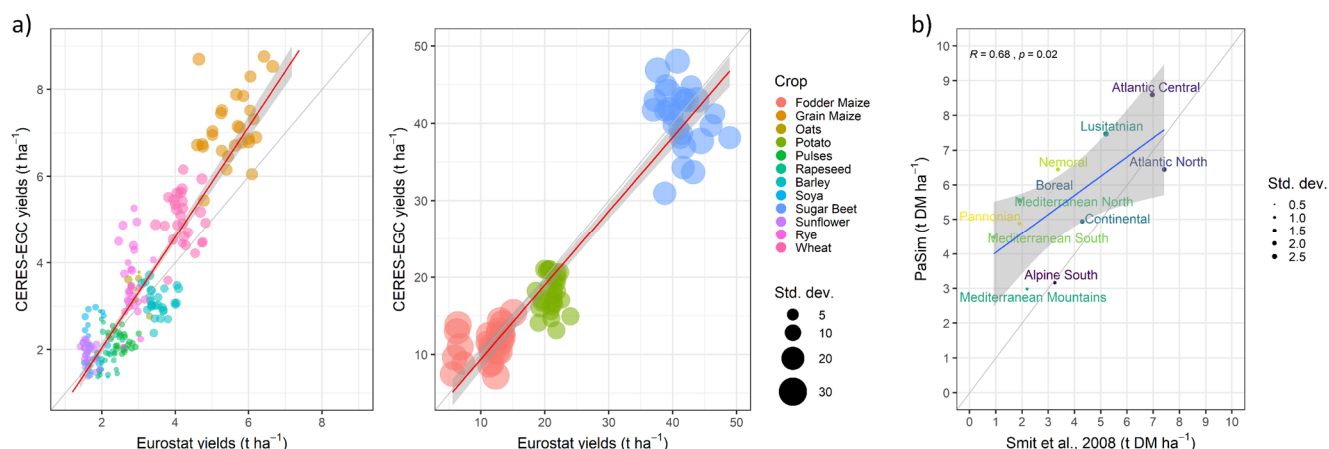
Figure 1: a) Simulated crop yields compared with Eurostat statistics in the period 1978-2004; yields are reported as standard humidity. b) Grassland production compared to Smith et al. (2008) for the period d 1995-2004. Point size represents the standard deviation (Std. dev.) of the simulated productions.

Smit et al. (2008) computed the production of permanent grassland (pastures and meadows) across Europe based on national and international statistics for the period 1995-2004. The productivity simulated with PaSim (Fig. 1b) and aggregated to NUTS2 level (257 regions in this study) shown a significant positive spatial correlation (r = 0.68, p < 0.05) with the statistics reported by Smit et al., 2008, following the environmental stratification of Europe (Metzger et al., 2005). Compared to these statistics, PaSim scored a RMSE of 2.37 t DM ha^{-1} y^{-1}, a MAE of 2.04 t DM ha^{-1} y^{-1} and a negative E (-0.34). Simulated productivity was generally overestimated in the Mediterranean area (+55 %; representing 16 % of the surface) and East Europe

(+20 %; representing 25 % of the surface). A slight underestimation of the simulated productions was recorded for the Atlantic North zone (-15 %; representing 8 % of the surface). Finally, livestock densities and distribution were in line with the Eurostat findings at country scale for the period 1995-2004, ranging from 0 to 1.35 LSU ha^{-1} (mean: 0.34 LSU ha^{-1}). Livestock densities were higher in Belgium, the Netherlands, Denmark and Ireland, and in some regions of Germany, France, Italy and Spain, as also reported by Lesschen et al., (2011). Further details are reported in the supplementary material S.3.

3.1.2 Effects of climate change scenarios on productive systems

Our results showed increasing cropland and grassland productions in Europe during the historical scenarios (Fig. 2). Productions were positively correlated with the increasing air temperatures over this period. Mann–Kendall test highlighted a positive linear increase ($p \ll 0.01$) in the mean annual maximum air temperature (0.05 °C year^{-1}) and minimum air temperature (0.04 °C year^{-1}), as well as in solar radiation (0.02 MJ m^{-2} year^{-1}).

Crop production in Europe assumed a positive yearly increase during the historical period (18.1 kg DM ha y^{-1}; Fig. 2a), which persisted until 2020, reaching 4.6 t DM ha^{-1} (average 2005-2020). Compared to the historical period, crop production raised in the first part of the century for both climatic scenarios (+5 %; Table 1), even if the rate of increase slow over time, especially from year 2020 to 2050. In the second part of the century, crop production remained stable for the scenario RCP4.5 (+2 % compared to the average of the historical period), while a reduction of -6 % is forecasted for the RCP8.5 scenario; this decline reached -13 % in the end of the century (period 2080-2099). The extension of irrigation to all European croplands foster crop productions to +10 % in the first half of the century, while in the second part of the century crop productions were sustained only for RCP4.5 and irrigation mitigates the projected decline for RCP8.5 (+2 % compared to historical period).
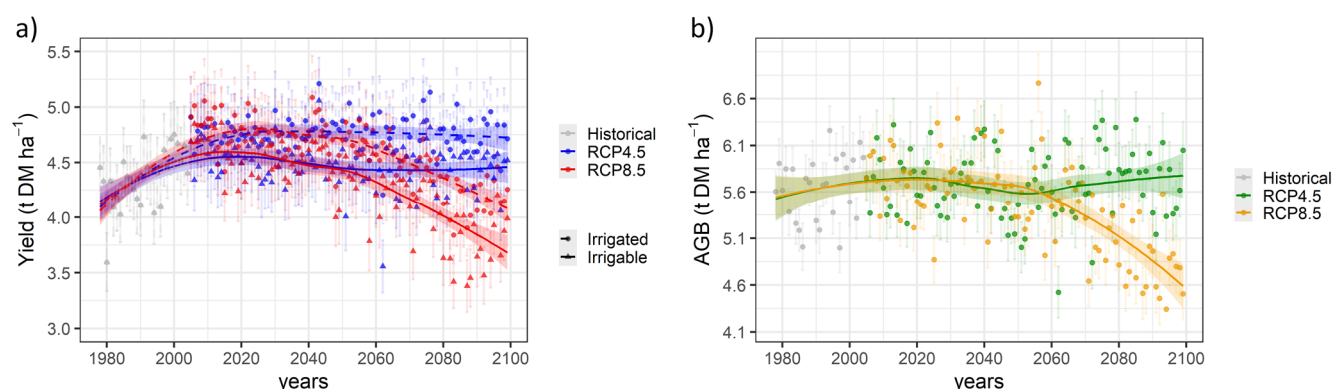
Figure 2: a) Crop yield trends in Europe from 1978 to 2099 with the two climatic scenarios RCP4.5 and RCP8.5, and two irrigation conditions following the irrigable agricultural area in Europe or extending the irrigation to all the arable lands (i_RCP4.5 and i_RCP8.5); all crops confounded. b) Grassland yield reported as the sum of biomass mowed and ruminant intake.

Crop production showed a clear trend over latitudes and over time. During the historical period, crops were more productive in low latitudes (< 45°) than in mid latitudes (45°-55°; -25 % compared to low latitudes, p >> 0.05) and higher latitudes (>55°;

300   -46 % compared to low latitudes, p >> 0.05). These gaps were reduced during the climate scenarios (Table S1). In low latitudes yields were comparable with the historical period in the first half of the century, undergoing to severe reductions towards the end of the century (-4 % and -11 % for RCP4.5 and RCP8.5, respectively). Moving to mid and to high latitudes crop productions increased in the first part of the century for both climatic scenarios (from +5 to +12 %). In the second part of the century, productivity was maintained only for mid latitudes in the RCP4.5 (+3 %), whereas declined for the RCP8.5 scenario (-8 %).

305   High latitudes were characterised by a further increase towards the end of the century (+14 % and +12 % for RCP4.5 and RCP8.5, respectively).

The yield of the two most cultivated crops in terms of area in Europe, grain maize and winter soft wheat, were not negatively affected by climate perturbations in first half of the century with the RCP4.5 scenario, while a slight increase is expected in the RCP8.5 for grain maize (+2 %; average 2030-2049) and a decreased for winter soft wheat (-4 %). Drastic reductions are

310   projected for grain maize yield in the end of the century for both climate scenarios (-5 % in RCP4.5 and -19 % for the RCP8.5, average 2080-2099). Conversely, production is expected to increase for winter soft wheat for RCP4.5 (up to +8 %), and a decline (-1 %) for RCP8.5 (Fig. S2a,b). The adoption of irrigation for all European croplands increased the productivity of grain maize compared to the irrigable scenario (+8 % toward mid-century for both scenarios; +13 % and +16 % toward the end of the century for i_RCP4.5 and i_RCP8.5, respectively). On the other hand, small yield increases are expected with the

315   irrigation scenario for winter soft wheat.

Fig. 3 reports the length of the growing season for grain maize and winter soft wheat, underlining a consistent reduction during both climatic scenarios. Crop growing cycle considers that sowing dates were modulated according to climatic conditions. Compared to the historical period, in the middle of the century there was an average reduction of the growing season of -8 days for grain maize (-12, -5 and +9 days for low, mid and high latitudes, respectively) and -20 days for winter soft wheat (-

320   20, -19 and -6 days for low, mid and high latitudes, respectively). This trend remained constant for RCP4.5 scenario toward 2100, whereas worsened for RCP8.5, with averaged reductions of -27 and -36 days for grain maize and winter wheat, respectively. Severe reductions are expected at mid and low latitudes for grain maize (-34 and -24 days), and at mid and high latitudes for winter soft wheat (-49 and -38 days). The length of the growing cycle for all the crop, except for potatoes and sugar beet, was reduced of -12 days in the middle of the century and reached -19 days in the second part of the century (Fig.

325   S3). Conversely, potato and sugar beet shown an extension of the length of the cropping cycle over time in all scenarios, especially during the end of the century.
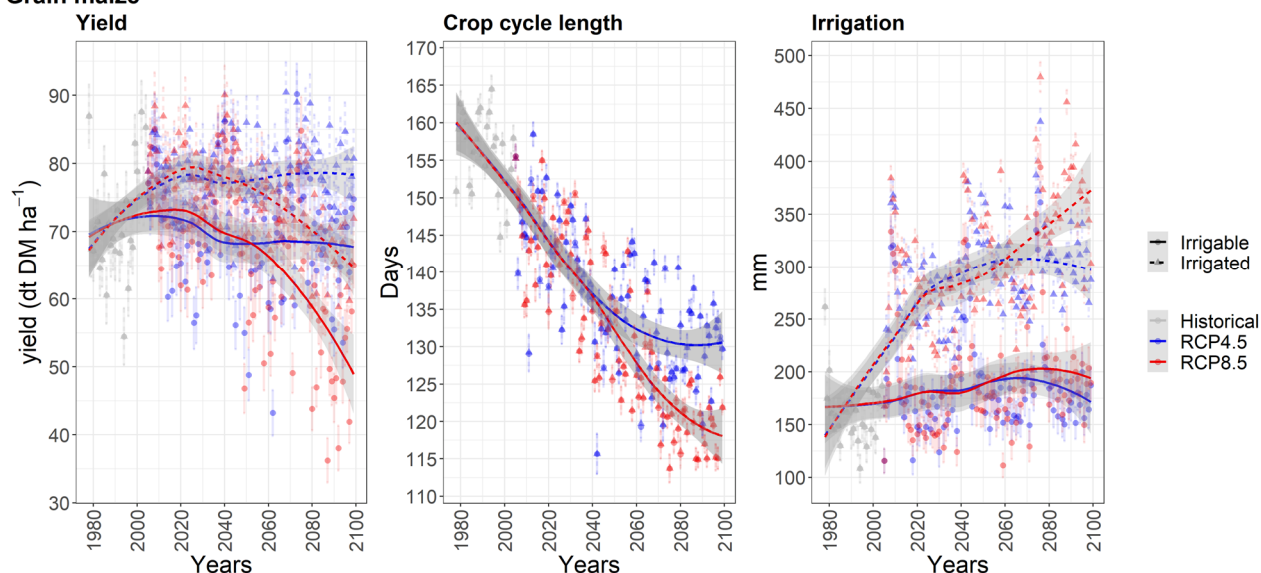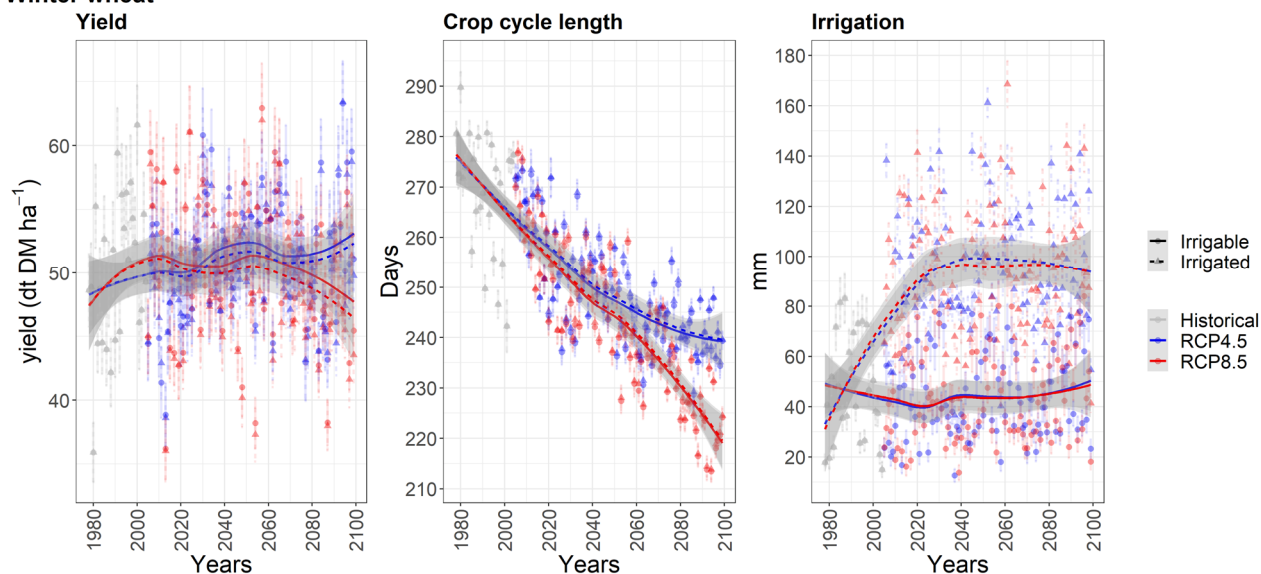
Figure 3: Yield, length of the cropping season and irrigation needed over the cropping cycle for fodder maize (a) and winter
330   soft wheat (b) in the two climatic scenarios RCP4.5 and RCP8.5; figure reports results for the European the irrigable area and
extension of the irrigation to all the European arable area (scenarios i_RCP4.5 and i_RCP8.5).

Considering the mild climate projections, positive yield increases from 4 to 20 % are expected for durum and soft wheat,
soybean, rye and spring wheat for low latitudes and toward the end of the century. On the other hand, grain and fodder maize,

potatoes, barley, sugar beet, pulses and oats, are affected by substantial reductions (from -1 % to -44 %). The extension of
irrigation is able to increase yields for the more water demanding crops (grain and fodder maize, sunflower, sugar beet and
potatoes) with increases of more than +10 %. At mid latitudes strong reductions, in the range of -2 to -17 %, are expected for
the large part of the main European crops (durum and soft wheat, potatoes, rapeseed, barley, soybean, spring soft wheat, sugar
beet, and sunflower), whereas fodder maize and winter rye were projected to increase (+30 and +9 %, respectively). High
latitudes displayed reductions in yields for pulses and barley (-22 % and -11, respectively), and an increase (+7 to over +100
%) for rapeseed, sugar beet, potatoes grain and fodder maize. The extension of irrigation to all European croplands will not
make sensible improvement for mid and high latitudes yields for i_RCP4.5, while a substantial reduction is projected for all
the crops in i_RCP8.5.

Table 1: Emissions of N_2O, CH_4, the net ecosystem production (NEP; for signs convention, negative values represent a stock
of carbon), and productivity from grassland and croplands. Between brackets is standard deviation.

Scenario and Period		N_2O		CH_4		NEP		Productivity[a]	
		Mean	Rate	Mean	Rate	Mean	Rate	Mean	Rate
		kg N-N_2O ha^{-1} y^{-1}	g N-N_2O ha^{-1} y^{-1}	kg C-CH_4 ha^{-1} y^{-1}	g C-CH_4 ha^{-1} y-1	kg C-CO_2 ha^{-1} y^{-1}	g C-CO_2 ha^{-1} y^{-1}	kg DM ha^{-1} y^{-1}	g DM ha^{-1} y^{-1}
Period 1978-2004									
Historical	Grassland	0.81 (0.1)	2.4	6.71 (0.4)	15.6	-622 (62)	-774	5635 (250)	9202
	Cropland	1.44 (0.2)	2.2			-3403 (214)	251	4359 (297)	18107
Period 2005-2049									
RCP4.5	Grassland	0.92 (0.1)	3.6	6.80 (0.4)	-6.2	-524 (65)	432	5697 (271)	-3457
	Cropland	1.52 (0.2)	1.3			-3505 (217)	-3268	4578 (313)	-2598
i_RCP4.5	Cropland	1.55 (0.2)	1.7			-3703 (225)	-4650	4815 (322)	393
RCP8.5	Grassland	0.92 (0.1)	3.4	6.76 (0.4)	-7.2	-519 (66)	995	5713 (274)	-1524
	Cropland	1.57 (0.2)	2.9			-3542 (215)	1441	4600 (314)	-7723
i_RCP8.5	Cropland	1.59 (0.2)	3.0			-3740 (223)	-111	4832 (322)	-5167
Period 2050-2099									
RCP4.5	Grassland	1.05 (0.1)	0.5	6.71 (0.5)	4.3	-526 (71)	149	5695 (288)	5411
	Cropland	1.66 (0.3)	3.6			-3472 (211)	-1661	4454 (304)	1567
i_RCP4.5	Cropland	1.64 (0.2)	2.4			-3713 (222)	-455	4775 (314)	-471
RCP8.5	Grassland	1.21 (0.1)	7.4	6.13 (0.4)	-23.7	-298 (65)	6407	5201 (285)	-21777
	Cropland	1.93 (0.3)	10.0			-3293 (210)	9838	4094 (277)	-16171
i_RCP8.5	Cropland	1.96 (0.3)	11.7			-3529 (221)	9488	4445 (290)	-13988

[a] Yield for croplands; the sum of harvested biomass and animal intake for grasslands.

Irrigation was applied to 93 % of all the simulation units, doubling the volumes needed to fulfil the evapotranspiration deficit
(160 mm y^{-1} in the first half of the century) compared to the historical period (82 mm y^{-1}). Then, water volumes needed in the
second half of the century are reduced for i_RCP4.5 (114 mm y^{-1}) and are slightly increased for i_RCP8.5 (176 mm y^{-1}).

Compared to the scenario with actual irrigable surface these volumes increased by more than 2 and 5 times at mid and high latitudes and only by +30 % at low latitudes, indicating that the extension of irrigable areas became an essential to ensure adequate levels of crop production, especially in the Mediterranean regions.

355 Grassland productivity showed a trend over time similar to croplands (Fig. 2b; Table 1). Compared to the historical period, grassland productivity slightly increased until 2020 to decline toward the middle of the century, with an average production of 5.6 t DM ha^{-1} (average 2030-2049). Biomass productivity is maintained during the progress of the RCP4.5 scenario, whereas an averaged reduction of about 0.45 t DM ha^{-1} (-7.7 % compared to the historical period) is expected for the RCP8.5 scenario in the second part of the century. During the historical period, grassland productivity at low latitudes was about 30 % lower

360 compared both to mid and high latitudes, with higher of productions concentrated in the north-west Europe. A substantial increase of production was observed toward 2050 both for low latitudes (+9 % for RCP4.5 and +10 % RCP8.5) and high latitudes (+13 % and +14 % for RCP4.5 and RCP8.5, respectively; Fig. S2c and Table S1 in the supplementary material). Moving to the end of the century, grass production increased further compared to the historical period, especially for RCP4.5 (+16 % and +22 % for low and high latitudes, respectively), while a less marked increase is expected for RCP8.5 (+6 % and

365 +13 % for low and high latitudes, respectively). At central EU latitudes, characterised by a higher livestock density than low and high latitudes (+42 % and +13 %, respectively), productivity was reduced of -6 % in RCP4.5 and -5 % in RCP8.5 in the middle of the century. This reduction remains constant for the RCP4.5 scenario toward the end of the century and was more pronounced for RCP8.5 (-24 %).

3.2 GHG emissions

370 ### 3.2.1 N$_2$O emissions
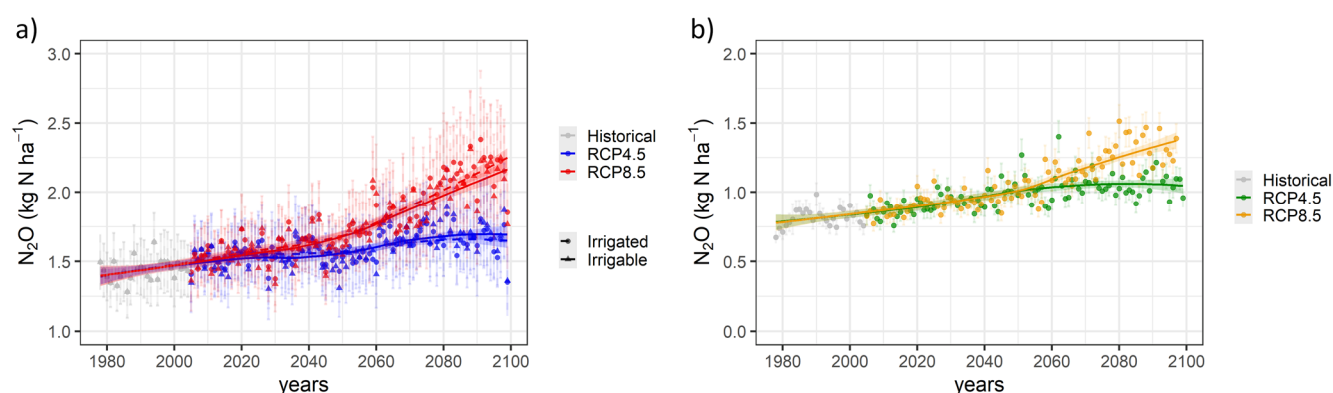
Figure 4: a) N$_2$O emissions (kg N ha^{-1} y^{-1}) for croplands and b) grassland with two climate change scenarios (RCP4.5 and RCP8.5). N$_2$O emissions for croplands consider two irrigation conditions, following the irrigable agricultural area in Europe or extending the irrigation to all the arable lands (i_RCP4.5 and i_RCP8.5).

375

N$_2$O emissions increased sharply for croplands along the century for both climate scenarios (Fig. 4a). During the historical period, a stable growth of the emission at the rate of 2.2 g N-N$_2$O ha^{-1} y^{-1} is observed, with a mean value of 1.44 kg N-N$_2$O ha^{-1} y^{-1} (Table 1). This rate decreased to 1.3 g N-N$_2$O ha^{-1} y^{-1} in the first half of the century for RCP4.5 scenario, while a rise of 2.9 g N-N$_2$O ha^{-1} y^{-1} is forecasted for the RCP8.5 scenario. In the second part of the century, the rate of emission was nearly

380   tripled for RCP4.5 compared to the emission in first half of the century. A strong increase of emissions is observed for RCP8.5, with a rate of 10 g N-N$_2$O ha^{-1} y^{-1}, reaching a mean of 2.09 kg N-N$_2$O ha^{-1} (average 2080-2099). RCP4.5 scenario, instead, reach a total of 1.69 kg N-N$_2$O ha^{-1}. The extension of irrigation to all European croplands amplified the emission rates in the first half of the century for both i_RCP4.5 and i_RCP8.5, compared with the irrigable scenario (+3 % and +26 %, respectively). Emission rates decreased in the second part of the century for i_RCP4.5 (-34 %), whereas grown up to +17 % for i_RCP8.5.

385   Furthermore, the interannual variance of N$_2$O emissions increased from the historical period to the first half of the century (+15 % in both scenarios) and continued for the second part of the century (+41 % and +75 % for RCP4.5 and RCP8.5, respectively). While, the extension of irrigation was able to reduce the interannual variance both i_RCP4.5 and i_RCP8.5 scenarios (+17 % and +61 %).

N$_2$O emissions from grasslands described a similar trend over the years as for croplands (Fig. 4b), characterised by lower rates.

390   During the historical period, the emission increased at a rate of 2.4 g N-N$_2$O ha^{-1} y^{-1}, with a mean value of 0.81 kg N-N$_2$O ha^{-1} y^{-1} (Table 1). The rate raised to about 3.6 g N-N$_2$O ha^{-1} y^{-1} during the first half of the century, afterwards the two different climate scenarios shown different trends. RCP4.5 was characterised by a significant reduction of the emission rate to 0.5 g N-N$_2$O ha^{-1} y^{-1}, while the rate tripled for RCP8.5, reaching 1.32 kg N-N$_2$O ha^{-1} y^{-1} in the end of the century (average 2080-2099). A total emission of 1.05 kg N-N$_2$O ha^{-1} is expected for RCP4.5.

395
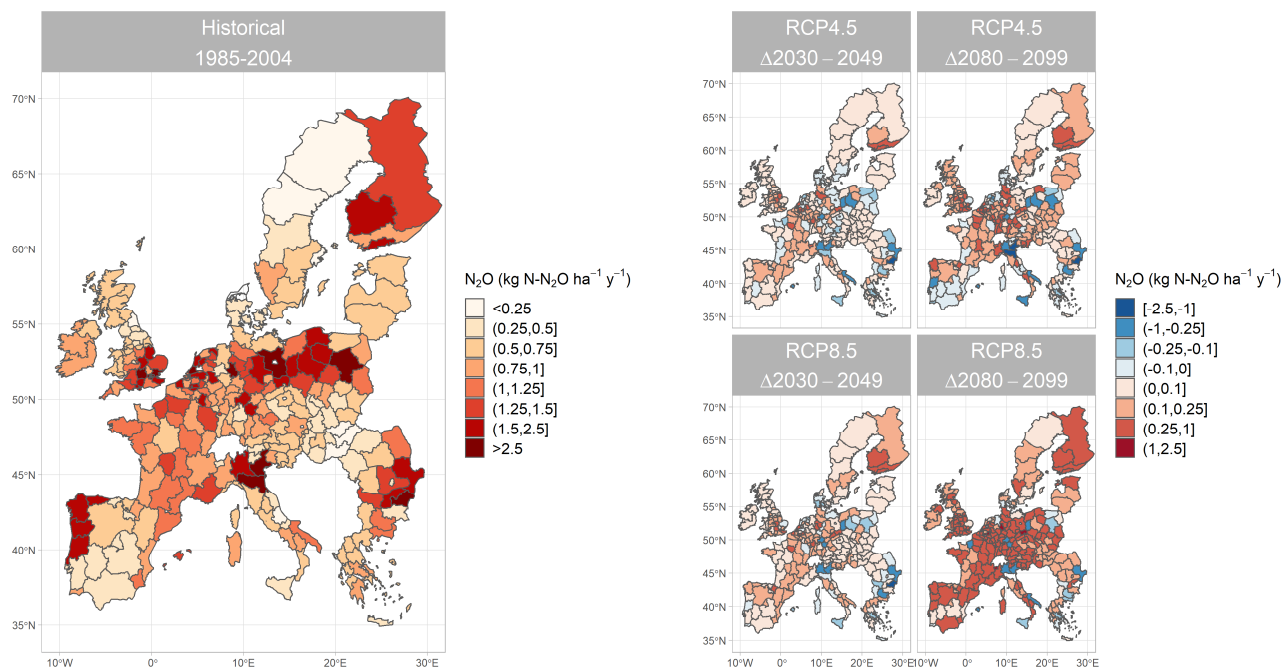
Figure 5: N_2O emission for croplands and grasslands in European administrative borders (NUTS2). Emissions are reported for historical period (1985-2004), and difference "Δ" with mid (2030-2049) and the end of the century (2080-2099) for the two climatic scenarios RCP4.5 and RCP8.5. N_2O emissions are reported in cropland with irrigable scenario (see the text).

400

Total N_2O emissions from cropland and grasslands were reported to the surface allocated for arable crops and permanent grasslands for each simulation unit, by using the share of Corine Land Cover inventory of 2018 (Fig. 5). Emissions ranged between 0 and 2.5 kg N ha^{-1} y^{-1} and were concentrated in hotspots, such as northern Italy, north-east Germany and Poland, southern England, Bulgaria, eastern Romania, the Scandinavian peninsula, the north-western of Spain and Portugal. During

405 the climatic projections is observed a general worsening of N_2O emissions towards the end of the century, reaching up and often over ±1 kg N ha^{-1} y^{-1}, especially for the strongest climatic scenario. An average of 1.02 kg N-N_2O ha^{-1} y^{-1} (corresponding to 0.163 Mt N-N_2O y^{-1}) were emitted during the historical period. This amount raised 1.06 and 1.08 kg N-N_2O ha^{-1} y^{-1} (0.166 and 0.170 Mt N-N_2O y^{-1}) in the first half of the century for RCP4.5 and RCP8.5, respectively. In the second half of the century total N_2O emissions assumed a further increase to 1.11 and 1.13 kg N-N_2O ha^{-1} y^{-1} (0.169 and 0.174 Mt N-N_2O y^{-1}) for RCP4.5

410 and RCP8.5, respectively.

The N_2O emission factor (EF), intended as the ratio between the N emitted as N_2O from croplands and grasslands, and the N introduced into the system (not including the N added by animal excretion, crop residue, atmospheric deposition, soil mineralisation and fixation), assumed the same trend described for N_2O over time. During the historical period the averaged EF for croplands was 1.88 % ± 0.32 %, while the EF for grasslands was 1.99 % ± 0.16 %, see Fig. S4a,b.

415
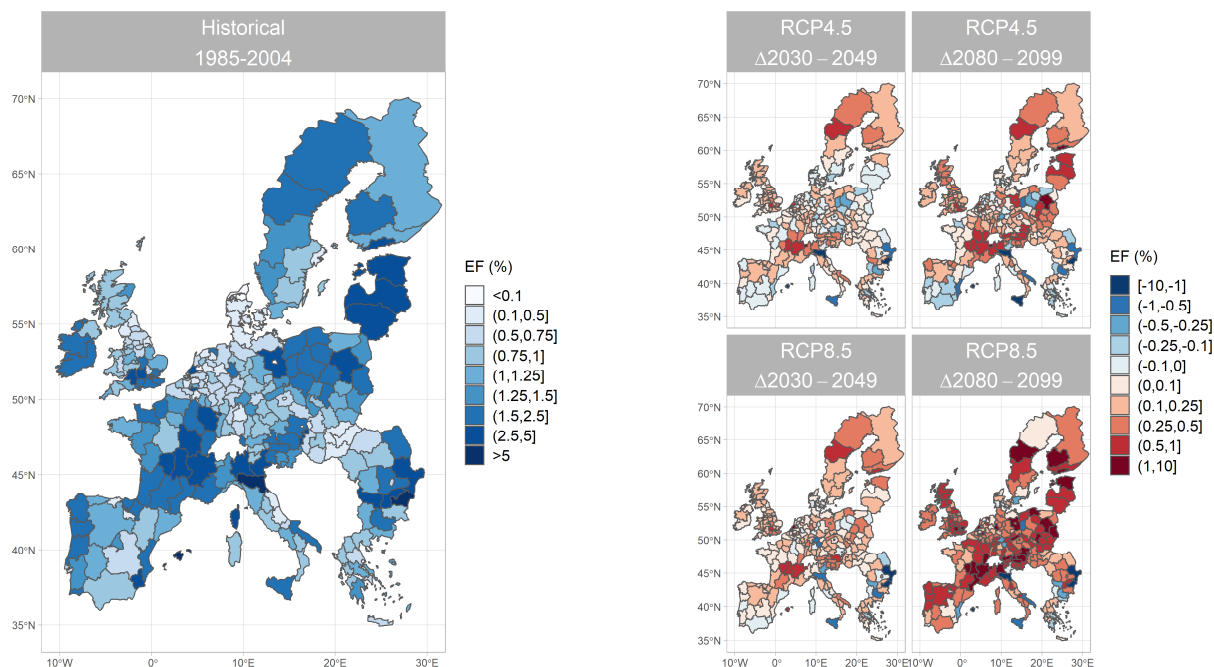
Figure 6. N₂O emission factor (EF %) for croplands and grasslands in European administrative borders (NUTS2). EF is reported for the historical period (1985-2004), and the difference "Δ" with the middle (2030-2049) and the end of the century (2080-2099) for the two climatic scenarios RCP4.5 and RCP8.5. EF is calculated as ratio between the N emitted as N₂O from croplands (irrigable surfaces) and grasslands, and the N introduced into the system (not including the N added by animal excretion, crop residue, atmospheric deposition, soil mineralisation and fixation).

Combining cropland and grassland emissions over each simulation unit, the resulting EF was 1.82 ± 0.07 % during the historical period, and rose to 1.90 ± 0.09 % for RCP4.5 and 1.94 ± 0.09 % for RCP8.5 in the first half of the century. EF was 2.02 ± 0.11 % and 2.05 ± 0.11 % for RCP4.5 and RCP8.5, respectively, in the second part of the century. The spatial distribution of EF values at NUTS2 scale, as reported in Fig. 6, varies from 0.1 % to over 5 % in the historical period, to assume variations between ±1 % in RCP4.5, and up to ±10 % in RCP8.5. The hotspots are the same described for the N₂O emissions. The specific EF for the simulated crops, calculated in the period from sowing (including pre-sowing management) to the sowing of the next crop in a succession (excluding pre-sowing management), ranged from 0.9 % to 3.4 % in the historical period, and is reported in Fig. 7. EFs toward mid- and the end of the century raised for all the crops, with a greater impact for the RCP8.5 scenario, except for winter soft wheat, which exhibited lower EFs values over the century, and soybeans which presented a low EF at the end of the century for RCP8.5 scenario compared to the less strong scenario. Fig. 7 reported the EF for N₂O also for grasslands, which assumed an increasing behaviour following the course of the century and the strength of climate scenarios.

435
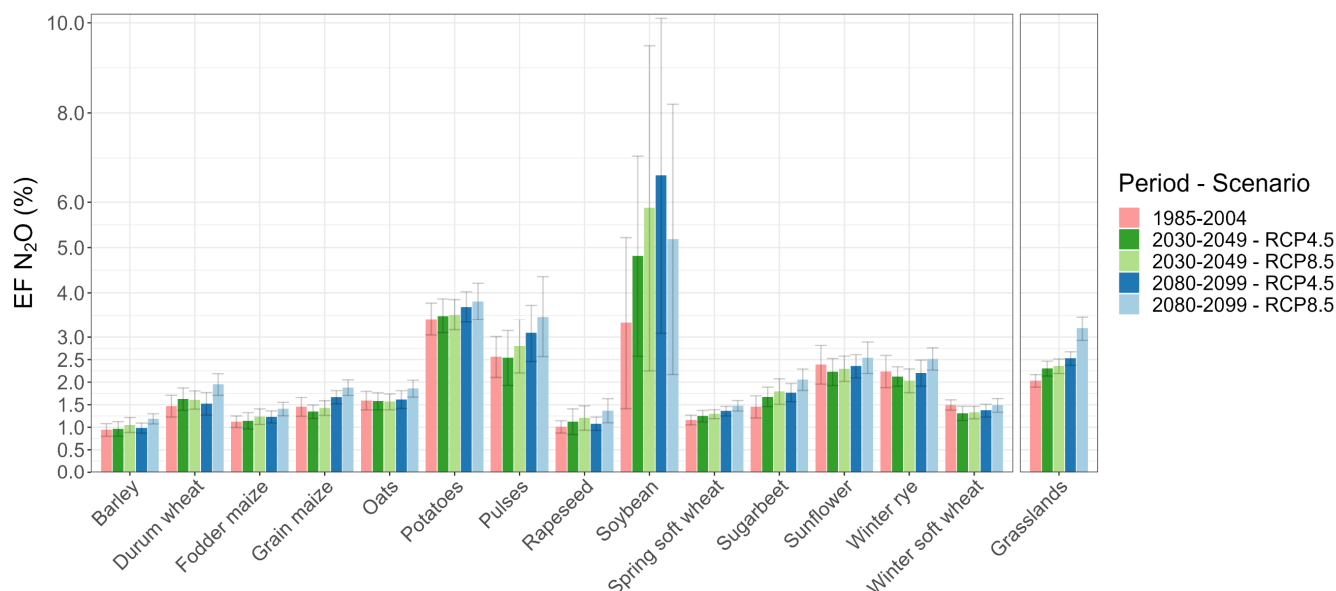
Figure 7: Emission factor (EF) for N₂O (%) for the different crops and grasslands for historical period (1985-2004), toward mid-century (2030-2049) and toward the end of the century (2080-2099), for the two climatic scenarios RCP4.5 and RCP8.5. EF is ratio between the N emitted as N₂O from crops and grasslands, and the N applied.

3.2.2   CH₄ emissions

440   The emissions of CH₄ from enteric fermentation are reported in Fig. 8. During the historical period, a mean emission of 6.71 kg C-CH₄ ha⁻¹ y⁻¹ was observed, with a rate of 15.6 g C-CH₄ ha⁻¹ y⁻¹ (Table 1). The emission rate halved in the first part of the century, to increase slightly in the second part of the century for RCP4.5 (4.3 g C-CH₄ ha⁻¹ y⁻¹) and strongly decrease for RCP8.5 scenario (-23.7 g C-CH₄ ha⁻¹ y⁻¹). Emissions toward the end of the year were 6.73 kg C-CH₄ ha⁻¹ y⁻¹ in RCP4.5 (average 2080-2099), and 5.74 kg C-CH₄ ha⁻¹ y⁻¹ for RCP8.5. The averaged CH₄ emissions per head ranged from 2.99 kg CH₄ head⁻¹ y⁻

445   ¹ in the historical period to reach 3.03 and 3.01 kg CH₄ head⁻¹ y⁻¹ In the first half of the century for RCP4.5 and RCP8.5, respectively. In the second half of the century a reduction to 2.98 and 2.73 kg CH₄ head⁻¹ y⁻¹ are expected for RCP4.5 and RCP8.5, respectively. The spatial distribution of CH₄ emissions at NUTS2 scale is reported in Fig. 9 and ranged from 0 to over 20 kg C-CH₄ ha⁻¹ y⁻¹ in the historical period and resulted concentrated in the north-west part of Europe. During the climate projections, methane emissions assumed variations in the range of ±12 kg C-CH₄ ha⁻¹ y⁻¹, with increases mostly concentrated

450   in northern Europe.
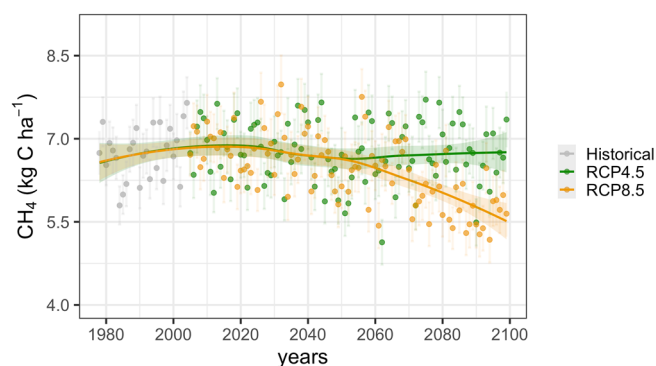
Figure 8: CH$_4$ emissions (kg C-CH$_4$ ha^{-1} y^{-1}) from enteric fermentation grasslands with two climate change scenarios (RCP4.5 and RCP8.5).
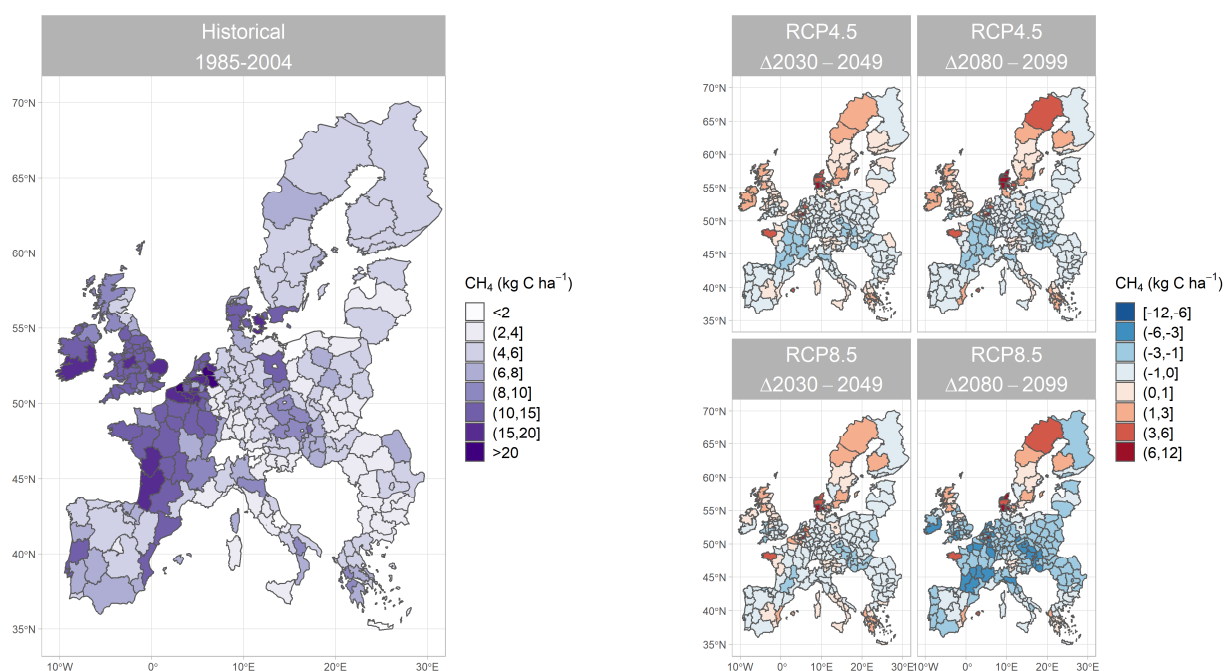
455 **Figure 9:** CH$_4$ emission for grasslands in European administrative borders (NUTS2). Emissions are reported for historical period (1985-2004), and difference "Δ" with mid (2030-2049) and the end of the century (2080-2099) for the two climatic scenarios, RCP4.5 and RCP8.5.

3.2.3 Carbon fluxes

460 Results are presented with sign convention indicating CO$_2$ accumulation as negative, and CO$_2$ losses as positive. Net Ecosystem Production (NEP) for European croplands showed a clear intensification of CO$_2$ accumulation until 2050. Rates

were contrasting for RCP4.5 and RCP8.5, -3.27 and +1.44 kg C-CO_2 ha^{-2} y^{-1}, respectively (Fig. 10a; Table 1). In the second part of the century, a net divergence between the trends of the two climate scenarios is expected. CO_2 is continuously accumulated for RCP4.5 (-1.66 kg C-CO_2 ha^{-1} y^{-1}), whereas a decumulation is projected for RCP8.5 (9.84 kg C-CO_2 ha^{-1} y^{-1}).

465   Extending the irrigation area over all European croplands, which taken advantage of irrigation volumes according to crop needs and soil water status, produced a proportional increase of CO_2 accumulation in the climatic scenarios for both the first half of the century (+6 %) and the second half (+7 %). NEP for croplands is expected to increase toward 2050 at low latitudes (+3 %) for both RCP4.5 and RCP8.5 (Fig. S5a; Table S1). This trend is inverted toward the end of the century for RCP4.5 scenario (-1 %), while turn to more severe for RCP8.5 (-8 %). In central European latitudes CO_2 is accumulated in the first

470   part of the century for both climate scenarios (+9 %) and tended to be released in the end of the century for RCP8.5 (-3 %). Compared to central European latitudes, higher latitudes shown a trend to store more CO_2 for the RCP4.5 scenario respect to the historical period (+5 % in the middle of the century and +9 % in the end of the century), whereas a tendency to release CO_2 is forecasted for the RCP8.5 scenario, especially toward the end of century (-5 %). The extension of irrigation to all European area showed a clear CO_2 loss towards the end of the century for low and mid latitudes, while a potential accumulation was

475   observed at high latitudes.
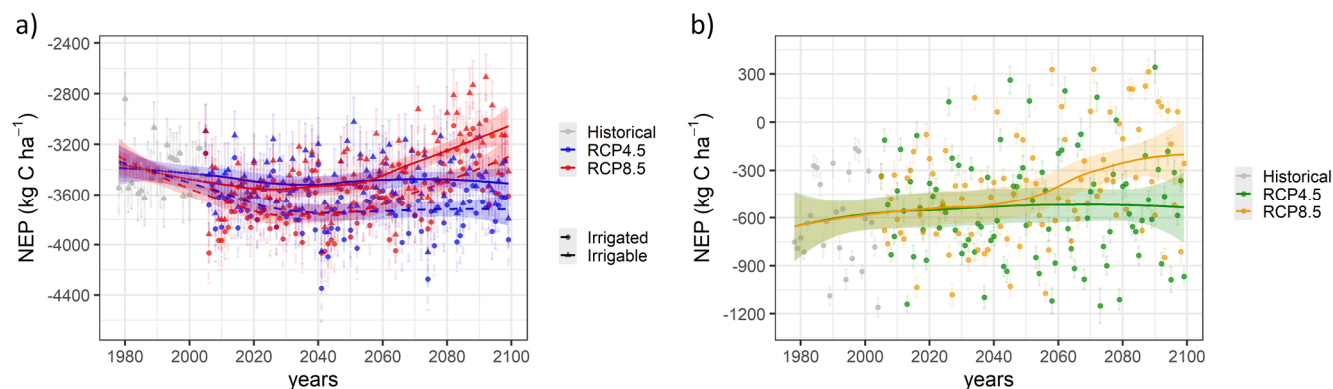
Figure 10: Net ecosystem production (NEP; g C ha^{-1}) for croplands (a) and grasslands (b), with two climate change scenarios (RCP4.5 and RCP8.5), and two irrigation conditions following the irrigable agricultural area in Europe or extending the irrigation to all the arable lands (i_RCP4.5 and i_RCP8.5)

480

NEP in grasslands indicated a clear trend to CO_2 accumulation into the system during the historical period (Fig. 10b; Table 1), with a rate of -0.77 kg C ha^{-1} y^{-1}. Towards 2050 a slight imbalance and a tendency to release CO_2 is observed for both climate scenarios. Towards 2100, the amount of CO_2 potentially stored into the system is maintained for RCP4.5 with a loss of about 100 kg C-CO_2 ha^{-1} y^{-1} compared to the historical period (-622 kg C-CO_2 ha^{-1} y^{-1}), while a clear tendency to CO_2 release was

485   forecasted, on average, for the scenario without adaptation, RCP8.5. In the second half of the century RCP8.5 scenario projected a potential loss of 50 % of the CO_2 annually stored in the historical period. A potential release of CO_2 is also projected for the RCP4.5 for low latitudes, both in the middle (-7 %) and towards the end of the century (-16 %), compared to the

historical period (Table S1). Higher decreases are forecasted for the RCP8.5 for the lower latitudes, -13 % and -37 % towards the first and the second half of the century, respectively. Conversely, for latitudes > 55° a potential storage of CO_2 is expected

490 for RCP4.5 (+2 % and +3 % for the mid and the end of the century, compared to the historical period), whereas the scenario RCP8.5 gain more CO_2 in the middle of the century (+2 %) and turns to negative (-31 %) toward the end of the century. The intermediate latitudes, corresponding to the central Europe, displayed a strong susceptibility to CO_2 release in both climatic scenarios, ranging between -19 % and -31 % for RCP4.5 in the middle and at the end of the century, respectively, and turning to more negative and equal to -50 % and -100 % for the RCP8.5 scenario (Fig. S5b).

495 NEP of the European cropland and grasslands system, obtained reporting emissions the surface allocated for arable crops and permanent grasslands in each simulation unit, is reported in Fig. 11. During the historical period, NEP varied between -7500 and +200 kg C-CO_2 ha^{-1} y^{-1} within the European regions. Climate projections showed variation up to ± 2800 kg C-CO_2 ha^{-1} y^{-1} from the historical values, identifying a tendency to store less CO_2 towards the first half of the century, especially for the Mediterranean regions. CO_2 stock is further reduced in central European latitudes towards the end of the century for RCP4.5

500 scenario, and came to a strong reduction on all regions during RCP8.5. A total of -1865 kg C-CO_2 ha^{-1} y^{-1} (corresponding to -338 Tg C-CO_2 y^{-1}) were stocked during the historical period. This amount raised in the first half of the century to -1845 kg C-CO_2 ha^{-1} y^{-1} (-336 Tg C-CO_2 y^{-1}) for RCP4.5 and -1859 kg C-CO_2 ha^{-1} y^{-1} (-339 Tg C-CO_2 y^{-1}) for RCP8.5. In the second half of the century NEP emissions assumed a further increase for both climatic scenarios to -1771 kg C-CO_2 ha^{-1} y^{-1} (-321 Tg C-CO_2 y^{-1}) for RCP4.5, and -1620 kg C-CO_2 ha^{-1} y^{-1} (-293 Tg C-CO_2 y^{-1}) for RCP8.5.

505 NGHGE indicated a potential capacity of the European production systems to store an average of -1155 ± 82 Tg C-CO_2eq y^{-1} during the historical period (Table 2). N_2O and CH_4 were able to offset the NEP by 6.2 % and 0.8 %, respectively. In the first half of the century, the NGHGE assumed a slight reduction for RCP4.5, indicating a potential C stock, whereas remained substantially unvaried for RCP8.5. In the second part of the century NGHGE increased for both RCP4.5 (-1087 ± 119 Tg C-CO_2eq y^{-1}) and RCP8.5 (-997 ± 159 Tg C-CO_2eq y^{-1}), indicating a slowdown of C accumulation. Irrigation scenarios highlights

510 an increased potential of C stock of about 3-4 %, mainly due to the greater NEP values. NGB indicated losses from European agricultural surfaces in the range of 236 ± 107 Tg CO_2eq y^{-1} for the historical period (Table 2). Losses increased both in the first and the second half of the century and for both climate scenarios, being higher for RCP4.5 than RCP8.5.
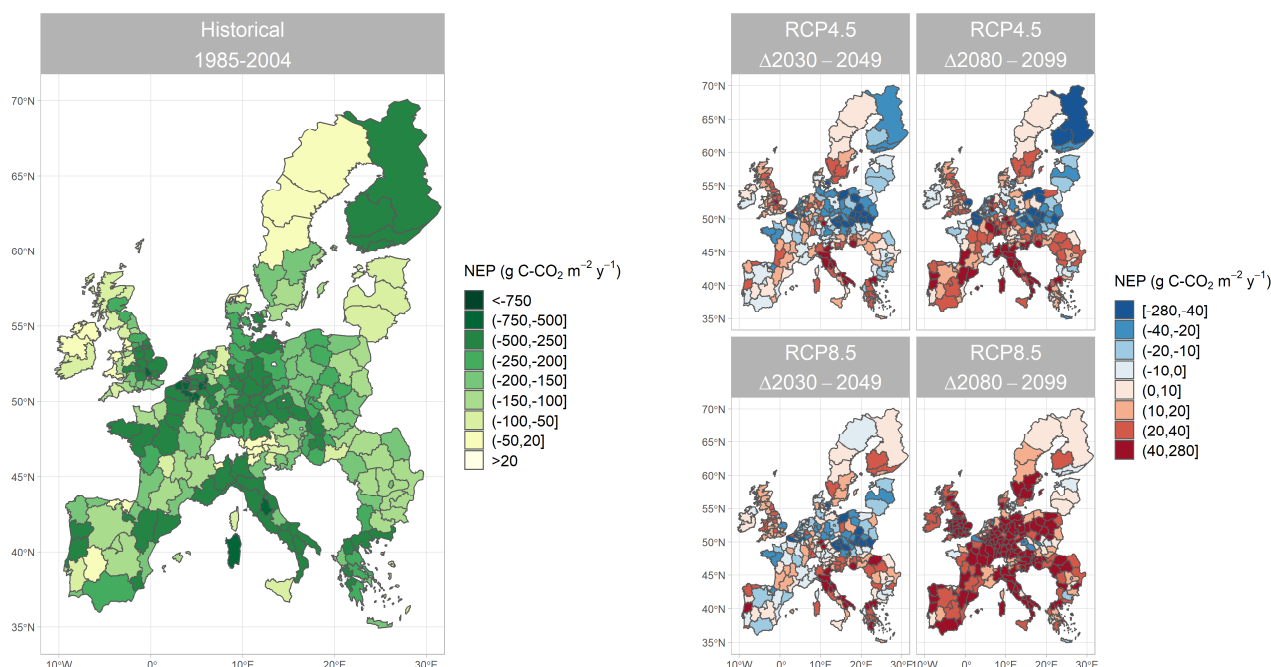
515 **Figure 11:** Net ecosystem production for croplands and grasslands in European administrative borders (NUTS2). Results are reported for historical period (1985-2004), and difference "Δ" with mid (2030-2049) and the end of the century (2080-2099) for the two climatic scenarios RCP4.5 and RCP8.5. NEP for croplands is reported with irrigable scenario (see the text).

520 **Table 2**: The net greenhouse gas exchange (NGHGE) and net greenhouse gas budget (NGB) in EUROPE during the historical and two climate change scenarios. The elements of the budget are reported: N_2O, CH_4 and the net ecosystem production (NEP; for signs convention, negative values represent a stock of carbon). Results are in Tg CO_2eq y^{-1}. Between brackets is standard deviation.

Scenario and Period	N_2O	CH_4	NEP	NGHGE	Harvest	Residues Exported	Fertilisation and dung	NGB
	Tg CO_2eq y^{-1}							
Period 1978-2004								
Historical	76.5 (3.4)	9.70 (0.9)	-1241 (82)	**-1155** (82)	1186 (63)	296 (26)	90 (3.5)	**236** (107)
Period 2005-2049								
RCP4.5	77.8 (3.6)	9.91 (0.9)	-1232 (113)	**-1144** (113)	1229 (78)	297 (22)	92 (4.5)	**290** (139)
i_RCP4.5	79.8 (3.1)	9.91 (0.9)	-1266 (103)	**-1176** (103)	1258 (67)	307 (22)	92 (4.5)	**298** (124)

RCP8.5	79.2 (4.5)	9.62 (0.9)	-1244 (104)	**-1155** (104)	1230 (73)	299 (22)	91 (4.5)	**282** (129)
i_RCP8.5	81.0 (4.5)	9.62 (0.9)	-1279 (99)	**-1189** (99)	1259 (65)	309 (23)	91 (4.5)	**288** (120)
Period 2050-2099								
RCP4.5	79.1 (5.2)	9.66 (1.1)	-1176 (118)	**-1087** (119)	1181 (87)	294 (22)	91 (4.6)	**297** (149)
i_RCP4.5	81.4 (4.7)	9.66 (1.1)	-1220 (104)	**-1129** (104)	1227 (73)	304 (21)	91 (4.6)	**311** (129)
RCP8.5	87.6 (6.2)	8.65 (1.2)	-1073 (159)	**-977** (159)	1072 (112)	286 (25)	89 (4.6)	**292** (197)
i_RCP8.5	90.8 (6.2)	8.65 (1.2)	-1114 (144)	**-1015** (144)	1121 (97)	293 (25)	89 (4.6)	**311** (175)

4 Discussion

4.1 Productions

Results from this study confirmed that the effects of climate change, implying shift of temperature, precipitation, and plant growing length among other factors, represents a serious drawback to plant production.

Air Temperature: Our findings pointed out that the increase of air temperature during the climate scenarios were negatively correlated with productivity, leading to a persistent reductions of biomass production in both grassland and croplands. This behaviour is confirmed also by previous studies (Challinor et al., 2014; Lobell and Tebaldi, 2014; Olesen and Bindi, 2002; Zhang et al., 2017), and was more pronounced for the more pessimistic climate scenario (-0.15 and -0.29 t DM ha^{-1} y^{-1} °C^{-1} for RCP4.5 and RCP8.5, respectively, in the 2050-2099 period). Effects of air temperature in the European crop yields ranges from +5 % to -11 % for every degree of rising temperature for both climatic scenarios (remaining negative along most of the climate projected scenarios: -1 % and -5 %, for RCP4.5 and RCP8.5, respectively in the period 2025-2099), as also reported by recent studies using modelling and multi-modelling approaches (*e.g.* Asseng et al., 2015: Bassu et al. 2014; Zhao et al., 2017; Yang et al., 2019). The extension of irrigable areas to all European croplands reduce the dependence of daily maximum and minimum air temperatures on crop production (Fig. S6). This demonstrates the fact that even with access to water (no limitation in irrigation), biomass production will decline due to increasing air temperatures, as reported by Minoli et al. (2019). This can be seen also from biomass projections in Fig. 2, considering an increase in temperatures over time. Interestingly, grassland productivity assumed a less pronounced correlation with air temperature during climate scenarios compared to croplands (Fig.12). RCP8.5, characterised by a strong reduction of grassland productions in the second half of the century, has an evident negative correlation with minimum and maximum daily air temperatures (r = -0.6, p < 0.01), up to a null correlation under RCP4.5. Furthermore, crop yields were strictly correlated with minimum and maximum air temperatures (r = 0.64 and r = 0.57, respectively; p < 0.01) compared to grasslands, which did not show such a dependence (r = 0.1 for both minimum and maximum air temperatures), highlighting a greater sensitivity of CERES-EGC model to air temperatures compared to PaSim.

Precipitation: Results confirmed that rainfall have a positive effect for both crop (r = 0.41 and 0.13 for RCP4.5 and RCP8.5, respectively; p < 0.01) and grassland production (r = 0.26 in RCP8.5, p < 0.01; null for RCP4.5). Compared to

550 the historical period, a reduction of precipitation was foreseen in the first half of the century for both scenarios (-2.1 mm y^{-1} for RCP4.5 and -0.74 mm y^{-1} for RCP8.5; p << 0.01) whereas in the second half of the century rainfall increases in RCP4.5 (+1.2 mm y^{-1}; p << 0.01) and decreases in RCP8.5 (-0.59 mm y^{-1}; p << 0.01). This effect was more pronounced for low latitudes (-1.2 and -2.3 mm y^{-1} for RCP4.5 and RCP8.5, respectively; p << 0.01) compared to high latitudes where the rainfall tends to increase during the century (+0.26 and +0.1 mm y^{-1} in RCP4.5 and RCP8.5, respectively, respect to the

555 historical period; p < 0.5). These expected reduction in cumulated precipitation, will negatively affect productivity with climate change scenarios, as confirmed by Hsu et al. (2012) for grasslands and by Olesen et al. (2011) for croplands.

Length of crop growing cycle: Apart from increases in temperature and reduction in precipitation, our simulation highlights that crop yield is affected by the shortening of the length of the growing cycle, as confirmed by Tao and Zhang. (2011), and Bassu et al. (2014). Bassu et al. (2014) predicted a general reduction of growing cycle length for maize in

560 central Europe with the multi-model assessment, de Souza et al. (2019) forecasted a reduction of 6 to 22 days for maize cultivation in RCP4.5, and up to 8 to 29 days in RCP8.5 for Brazil conditions by using DSSAT/CERES-Maize. The magnitude of reduction of the length of growing cycle for wheat is consistent with Yang et al. (2019) for the Mediterranean area which forecasted up to -26 days, compared to -22 days of our simulations. Our findings confirm that climate change will have a regionally distributed impact (Howden et al., 2007; Challinor et al., 2014; Parry et al., 2005; Lobell and Tebaldi,

565 2014) even in scenario that include mitigation measures to offset climate change (RCP4.5), creating the possibility to the design cropping systems with multiple crops in a year. Furthermore, a certain number of crops can be cultivated in the Europe even in the worst climate scenario and can potentially yield higher productions than today at high latitudes, while a whole reduction in crop production is expected for low latitudes.
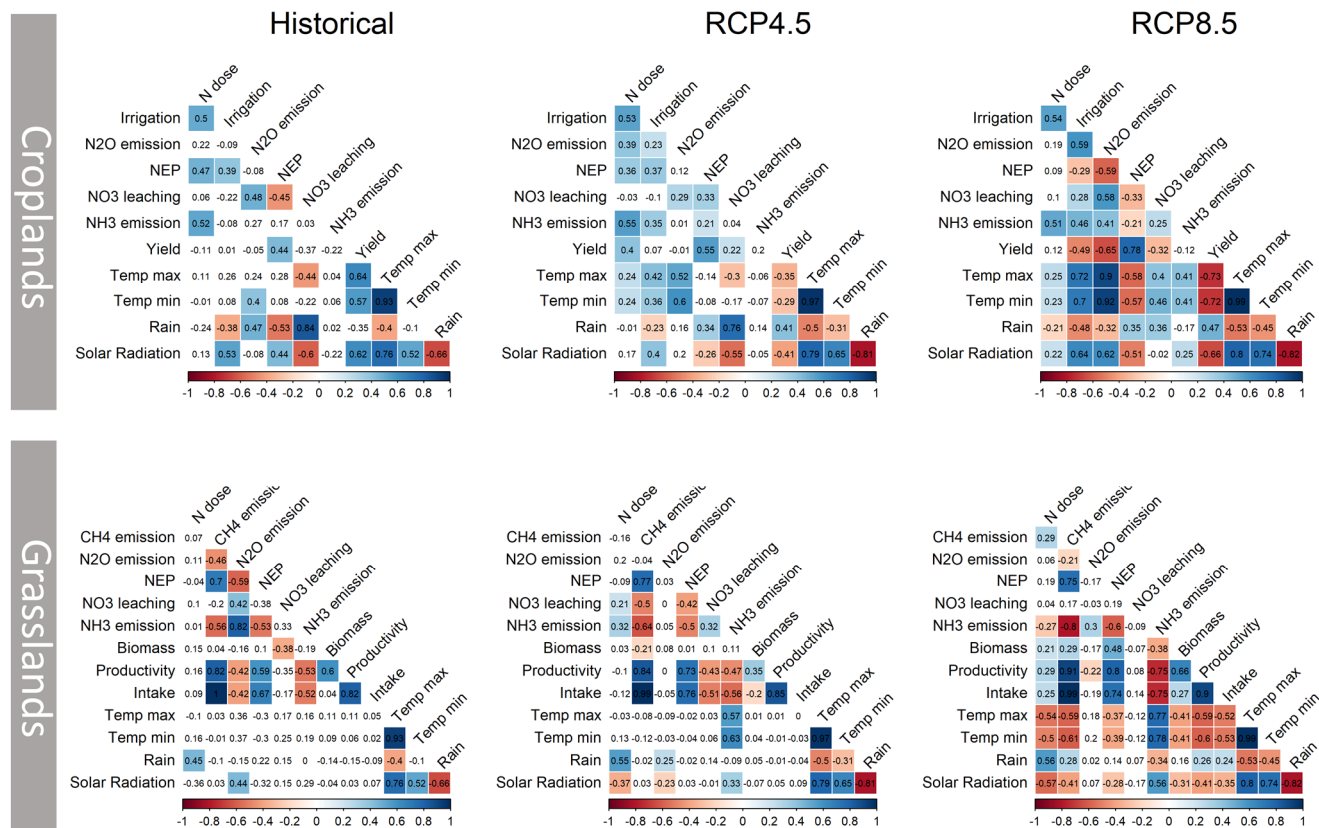
570   **Figure 12**. Correlation matrixes for croplands and grasslands considering the most interesting indicators for the objectives of this study. Correlation is presented for the historical period (1978-2004) and for the RCP4.5 and RCP8.5 scenarios; for croplands the irrigated and irrigable scenarios are reported in Fig. S6.

Finally, as reported in the result for the historical data (chapter 3.1.1), the productions of cropland and grasslands are in line

575   with available data and the recent, albeit scarce, literature, making this study coherent and representative. Regarding the climatic projections, our study predicted an average yield for croplands of 4.49 t DM ha^{-1} y^{-1} (ranging from 3.55 to 5.49 t DM ha^{-1} y^{-1}) in the period 2015-2099 with the RCP4.5 scenario, which is in line with the previous estimated yields reported by Lugato et al. (2018) of 4.34 t DM ha^{-1} y^{-1} (ranging from 3.69 to 4.90 t DM ha^{-1} y^{-1}) for the same period and climate scenario by using DayCent model.

580   Our study, assessing the effects of climate change in the European croplands and grasslands, give a support for the identification of climate smart practices. Among these, the modulation of crop sowing dates or the implementation of irrigation, represent possible solutions in the short to medium term to prevent water stress (Lehmann et al., 2013).

   Sowing date: Shifting sowing dates represents a promising adaptation to overcome yield drop (Olesen et al., 2012). Accordingly, our results showed that earlier sowing dates are expected for spring-sown crops under future climate

585   scenarios, compared to historical dates. Differences between historical and future sowing dates ranged from 0 to -5 days
      for both RCP4.5 and RCP8.5 scenarios towards 2050, whereas at 2100 horizon earlier sowing dates are predicted with
      differences of -5 and -7 days for RCP4.5 and RCP8.5, respectively. This clearly shows that the climate change allows
      significantly more advanced sowing in Europe, as confirmed by Tubiello and Rosenzweig (2008). For winter-sown crops,
      sowing dates extended in a range from +5 to +9 days toward 2050, to +13 days in the end of the century for RCP4.5. These
590   increases raised in RCP8.5, ranging from +7 to +13 toward 2050 and reaching +19 days on the way to 2100. The extension
      of irrigation in all simulated crops in Europe had a negligible influence on the length of the crop cycles, as discussed by
      Minoli et al. (2019), despite an increasing demand of water over the course of the century.

      Irrigation: Water demand has been shown to increase by +6 %, during the first half of the century, to slightly decrease in
      its second half for RCP4.5 (-2 %) and increase again for RCP8.5 (+23 %) scenario. These changes are in line with the
595   results of the multi-model approach used by Wada et al., (2013) analysing the uncertainty of the response of different
      hydrological models over Europe. Wada et al (2013) showed a decrease in water demand for irrigation toward 2100 of <5
      % for RCP4.5, and a rise of >20 % for RCP8.5 in Europe. Furthermore, from our study we observed that water demand
      would assume a strong regionally variation in Europe, with low latitudes needing 227 mm y^{-1} on average in the historical
      period (mean 1985-2004), an order of magnitude higher, respectively, than mid latitudes (29 mm y^{-1}) and high latitudes (9
600   mm y^{-1}). These proportions between the latitudes remained unvaried over the course of the century, whereas mid and high
      latitudes displayed a 20 % increase of water demand towards 2050 (mean 2030-2049) compared to historical period, in
      both climate scenarios. This phenomenon for low latitudes is strictly related to climate perturbation (*i.e.* strong increase of
      air temperature and reduction of rainfall), which increased crop water demand (Olesen et al., 2011). Furthermore, the
      potential increase of water demand even in mid and high latitudes, confirm that irrigation need to be supplied even for the
605   crops that are now commonly rainfed (*e.g.* spring and winter soft wheat, spring barley, sunflower, rapeseed). Towards
      2100, the water volumes needed for European croplands were largely reduced to under the amounts observed during the
      historical period, especially for low latitudes. These findings underline that even with high availability of irrigation water,
      the reduction of the crop growing cycle for the actual crop varieties, which sharpens toward the end of the century, is
      decisive to determine drops of yields. This is more evident for grain maize, the most water-demanding crop (Fig. 3), which
610   needs an additional +35 mm y^{-1} (average over Europe) to support production toward 2050, compared to the historical
      period. Towards 2100 water demand for maize remains identical to the historical period for RCP4.5, while increased (+25
      mm y^{-1}) for RCP8.5. Conversely, water demand for winter soft wheat remained constant along the century for both RCP4.5
      and RCP8.5 scenarios, whereas i_RCP4.5 and i_RCP8.5 scenarios confirmed an increasing water demand of about 50 mm
      (average over Europe; Fig. 3), as confirmed by Yang et al. (2019) for the Mediterranean regions.

4.2 Effect of climate on N_2O and CH_4 emissions

Emission of non-CO_2 GHG such as N_2O and CH_4 form enteric fermentation are strictly related to the trend of biomass productions (Maaz et al., 2021).

N_2O. The estimation and the projection of N_2O emissions in the historical and the climate change scenarios were in line with other model integrations over Europe. Lugato et al. (2017) estimated averaged emissions ranging from 1.18 to 2.63 kg N-N_2O ha^{-1} y^{-1} in the period 2010-2014 for both cropland and grasslands production systems with the DayCent model. In comparison with Lugato et al. (2017), we found similar results for the Mediterranean latitudes (about 1 kg N-N_2O ha^{-1} y^{-1}), while we predicted significantly lower emissions for Central Europe (1.1 kg N-N_2O ha^{-1} y^{-1}, this study), as well as at higher latitude (0.96 kg N ha^{-1} y^{-1}, this study), compared to 3 kg N-N_2O ha^{-1} y^{-1} forecasted by Lugato et al. (2017). Indeed, lower emissions at high latitudes were also reported by other studies (World Bank; Eurostat, 2017; Stehfest and Bouwman, 2006; Wells et al., 2018). Other research in the field were also within the range of our results *e.g.* Reinds et al., (2012) estimated emissions ranging from 1.1 to 2.4 kg N-N_2O ha^{-1} y^{-1} for arable lands for the year 2000, de Vries et al. (2011) 0.27 and 0.38 Mt N-N_2O y^{-1} for fertilizers and manure, and from grazing, respectively. Recently estimation by Eurostat (2017) reported values of 0.39 Mt N-N_2O y^{-1} (184.8 Tg CO_2eq) for the year 2015, based on lower Tier methodology, while our study reports lower values equals to 0.17 Mt N-N_2O y^{-1} (80 Tg CO_2eq) for the same year. Tian et al. (2020) reported emissions from EU agriculture based on global inventories in the order of 0.51 Mt N-N_2O y^{-1} in the decade 2007-2016, significantly higher than those found in our study (0.17 Mt N-N_2O y^{-1}) for the same period. In addition, the estimation by Tian et al. (2020) included also manure management and aquaculture, and suffers from high uncertainties given by the quality of the data and statistics used as input and, foremost, by the use of default emission factors. Regarding climate projection studies, Lugato et al. (2018) quantified N_2O emissions for croplands in the RCP4.5 scenario, reporting losses of 1.81 and 1.77 kg N-N_2O ha^{-1} y^{-1} for the first and the second part of the century, respectively. These estimations resulted comparable, while slightly higher, to the emissions for croplands issued from our study, both for the first part of the century (1.53 ± 0.23 kg N ha^{-1} y^{-1}) and for the second (1.66 ± 0.28 kg N ha^{-1} y^{-1}). Our study highlighted that crop type is a significant determinant of N_2O EFs of fertilisers, with most of the cereals having low EF (barley, fodder maize, soft spring wheat and rapeseed; mean = 1.1 %), and pulses, soybean and potatoes a high (mean EF = 3.1 %), during 1985-2004 integration period. The highest EF for leguminous crops indicates that the management of fertilisation for these crops, or for the rotation itself, can be improved on the input data. Finally, information about crop-specific EF turns to be useful to design crop successions and compiling emission inventories (Myrgiotis et al., 2019). However, our results were higher than the 1 % default value defined by the IPCC guidelines for the N applied to agricultural soils, mainly because we consider only the N applied as fertiliser, neglecting animal excretions, crop residues, deposition, mineralization and fixation. Anyway, this default factor shows large uncertainties at local to regional scales, especially for agricultural N_2O emissions, due to the scarce captured dependence of emission factors on spatial diversity of management, pedoclimatic, soil physical and biochemical conditions (Leip et al., 2011; Reay et al., 2012; Shcherbak et al., 2014; Cayuela et al., 2017). We observed

that N$_2$O emitted from croplands had a significant and positive correlation (p < 0.05) with rainfall (r = 0.47), as well as minimum and maximum air temperatures during the historical period (Fig. 12). The correlation with the minimum and

650   maximum air temperatures increased (p < 0.01) depending of the climatic scenarios (r > 0.5 for RCP4.5 and r > 0.9 for RCP8.5; Fig. 12), while the relation with rain turned to negative for RCP8.5 (r = -0.32, p < 0.01). This trend inversion is probably connected to the strict dependency of N$_2$O emissions to the length of crop growing period rather than the yearly cumulated rainfall, which can occur outside of the cultivation period, as also stated by Shcherbak et al. (2014). Accordingly, the correlation from N2O and the irrigation amount occurring during the cultivation period raised in the climate scenarios

655   (r = 0.23 and 0.59 for RCP4.5 and RCP8.5, respectively; p < 0.01). Moreover, N$_2$O emissions from cropland and grasslands were both positively correlated with soil clay content (> 0.5, p < 0.01; data not shown) for values lower than 32 %, as higher clay content can promote complete denitrification (Weitz et al., 2001).

CH$_4$. Methane emissions in EU were mainly concentrated in the regions with the highest density of grazing animals (Vuichard et al., 2007). The range of the emissions simulated in this study were in line with the simulation of Chang et al.

660   (2015), which found emissions of 18.7 ± 7.9 kg C-CH$_4$ ha^{-1} y^{-1} (period 1961-2010) and by Hörtnagl et al. (2018) by experimental trials from central European grasslands. Soussana et al. (2007) reported emissions over Europe higher then to our study, 41 kg C-CH$_4$ ha^{-1} y^{-1} with comparable animal densities, as well as Viuchard et al. (2007) with 108 kg C-CH$_4$ ha^{-1} y^{-1} using PaSim model, but with a higher stocking rate. CH$_4$ emissions decreased towards the end of the century, especially in the RCP8.5 scenario, due to reduced biomass productivity of grasslands that reduced animal intake (Fig. 2)

665   and the stocking density, which is reduced to 8 % compared to RCP4.5 in the last decade of the century. Reduction of stoking density was also found by Chang et al. (2015). Furthermore, rising temperatures and reduced precipitations could be able to decrease the protein content and the digestibility of the forage, resulting in a possible reduction of N$_2$O losses from dung and urine in pastures. However, this mechanism could be compensated by in an increase of methane (CH$_4$) losses (Wilkinson and Lee, 2017).

670   **Nitrogen Use Efficiency (NUE).** We observed an increase in the NUE for the European croplands, especially for the mild climate change projection. Compared to the historical period, in the RCP4.5 scenario, there is a reduction in the correlation between N$_2$O emitted with the other N losses (NO$_3$ and NH$_3$) and crop yield (Fig. 12). Conversely, there is an intensification of the dependence with the N dose. In fact, with an identical amount of N applied in the rotations over the simulated years, both NO$_3^-$ and NH$_3$ losses were reduced along the century (data not show), and crop yields increased, at least, until 2050.

675   This indicated a potential increase in the NUE. Kanter et al. (2016) observed an increase of the NUE by 2050 due to the increasing yields, support our findings. The improvement of NUE is a key factor to reduce environmental negative effects and mitigating GHG emissions. Bouwman et al. (2013) indicated that NUE improvement could reduce N$_2$O emissions by more than 30 % by 2050 in the RCP8.5 scenario. On the other hand, in the RCP8.5 scenario the correlation between N$_2$O emissions and N dose is lost (p > 0.01), and a strong negative (p < 0.01) score between yield and nitrogen losses took place,

680   indicating a reduction of NUE. This lack of relationship is most probably connected to the interannual variability of N$_2$O

emissions in the strongest scenario and in the second part of the century. Higher NUE are typical for low European latitudes than mid and high latitudes, since yields are generally higher and the N losses lower (Sutton et al., 2011). Improving actual agronomic practices to improve NUE could have several benefits. These practices can increase crop yields and reduces reactive N losses, including N_2O emissions (Lassaletta et al., 2014; Myrgiotis et al., 2019). In this context, irrigation

685   represents a fundamental intensification practice to counteract the effects of climate change in crop productions (Minoli et al., 2019). In our case, the extension of the irrigation to all cropping systems in EU significantly decreased N losses as (-5 % for NO_3 leaching and -4 % for NH_3 emissions, on average, for both i_RCP4.5 and i_RCP8.5 scenarios), and increased crop yield (Fig. 2), leading to a potential increase in the NUE.

Concerning grasslands, we noted weak relationship between N_2O emissions and N application doses. During the historical

690   period, N_2O emissions were positively correlated with NO_3 and NH_3 losses and negatively correlated with productions, representing a potential low NUE. Moreover, N_2O emissions in grassland were anti-correlated with CH_4 emissions. CH_4 emissions are rather positively related to biomass production and livestock intake. Therefore, low biomass production could potentially increase N_2O emissions, due to low NUE, and can decrease CH_4 losses, due to low livestock intake. Surprisingly, N_2O emissions in grasslands were weakly correlated with meteorological variables, especially minimum and

695   maximum air temperatures, whereas a relation with rain and solar radiation is noticeable for RCP4.5, while is not evident for RCP8.5. As observed for croplands, the relation between N_2O and NH_3 emissions is positive, especially for the RCP8.5 scenario, to indicate a possible reduction of the NUE.

4.3   Potential carbon stock

NEP. The NEP represents a simple indicator of carbon storage potential, since does not account for C removal in terms of

700   yield, animal intake or crop residues. Concerning cropland, our results are directly comparable with Kutsch et al. (2010) during the historical period who observed fluxes of -2400 ± 1130 kg C-CO_2 ha^{-1} y^{-1} based on field measurements in multiple sites in Europe (see Table 1), confirming a net potential storage of C. Regarding climate scenarios, a noticeable decline of C uptake was predicted in north-western cropping systems (British islands, Scandinavian peninsula) and Mediterranean area. This is most probably due, respectively, to the increase of soil heterotrophic respiration caused by

705   climatic factors, and to a potential reduction of NEP, as also reported by Kirschbaum (1995) (Fig. S7). Further decreasing values of NEP (towards carbon stock) were evident in the central and in the north-eastern European, especially in the first part of the century. A substantial decline of NEP in croplands was predicted towards the end of the century for the RCP8.5 scenario. This decline is most probably due to the low levels of heterotrophic respiration (*i.e.* microbial respiration due to soil organic matter decomposition processes) related to a partial soil coverage (*e.g.* cover crops) of the simulated crop

710   successions (Emmel et al., 2018). Conversely, in grasslands systems we observed lower averaged values compared to arable lands. This is related to the continuous biomass removal from grazers, the general higher content of SOC in the topsoil, the long-term land use (Morais et al., 2019), and the larger heterotrophic respiration that characterises these soils, especially if extensively managed (Bahn et al., 2008). These evidences were also described by Chang et al. (2015) who

historical period from our study). In general, areas where the heterotrophic respiration is enhanced by climatic drivers or by high amount of SOC, would lead to lower values of NEP (Chang et al., 2017). This is the case for the north-east of France and the British islands, while for the Scandinavian peninsula and north-east Europe, characterised by low C and low heterotrophic respiration, NEP reached higher values. These findings point out that in view of a growing productivity expected towards 2050, storing additional (new) carbon will be more challenging in areas characterised by high levels of SOC (Hassink and Whitmore, 1997), mainly due to high levels heterotrophic respiration. Finally, grasslands remained a potential sink for C during the historical period, which was in line with experimental measurements performed in the last two decades, *e.g.* -2470 ± 670 kg C-CO_2 ha^{-1} y^{-1} reported by Soussana et al. (2007), and -25 to -486 g kg C-CO_2 ha^{-1} y^{-1} reported by Hörtnagl et al. (2018). However, our results were slightly higher in absolute value than the mean value simulated by Cheng et al. (2015) from 1961 to 2010 (-570 ± 210 kg C-CO_2 ha^{-1} y^{-1}).

N_2O emissions from croplands were able to offset (reduce) the C sequestration potential. Offsets were in the order of 5.4 % for the historical period, and up to 6.1 % and 7.5 % in the end of the century for RCP4.5 and RCP8.5, respectively. The extension of irrigation to all European arable lands reduced these gaps, mainly due to the increase values of NEP (5.4 % and 7.1 % for i_RCP4.5 and i_RCP8.5). Few data are available in the literature regarding the CO_2 storage potential for croplands (Emmel et al., 2018). Our results confirmed that croplands may act as a potential sink of C when ignoring C exports by harvest (Buysse et al., 2017; Ceschia et al., 2010).

N_2O and CH_4 emissions in grasslands were able to offset NEP during the historical period by 17 % and 1 %, respectively. These results are compatible with the studies reported by Soussana et al. (2010) who displayed offsets over EU of 34 % and 10 % for N_2O and CH_4, respectively. During climate projection, the offset rises to 22 % for N_2O and 1.2 % for CH_4 towards 2050 for both RCP4.5 and RCP8.5. In the second part of the century N_2O emission offset the potential carbon sequestration by 26 % and 52 % for RCP4.5 and RCP8.5, respectively, while CH_4 offsets varied between 1.2 % and 1.9 % for RCP4.5 and RCP8.5, respectively.

4.4 GHG emission budget

For both cropland and grasslands, CO_2 storage potential (estimated from NEP) provided the largest term in the net greenhouse gas exchange balance (NGHGE), confirming the statement by Jones et al. (2016). The NGB, calculated as the balance between NGHGE and other C forms (*i.e.* harvest, manure and crop residues), indicated that European agricultural surfaces are a net C source. The most important components that determined these losses were the C exports, yield (F$_{C-harvest}$) and crop residues (F$_{C-residues}$), which varied proportionally to the NEP in the various climatic projections, *i.e.* the lower the NEP, the lower the yields. The non-CO_2 GHGs, despite being high especially in the RCP8.5 scenario towards the end of the century, had a minor impact in the differentiation of the two climatic scenarios, although they represent an important component in the overall carbon balance at the European level (see Table 3).

The values observed for NGB highlight that C inputs into the system such as organic fertilizers (the manures used in this study have a C:N ratio of 25 and represent 2/3 of the component $F_{C-manure}$), or actions aimed to recycle a portion of biomass in the field (crop residues management), are essential to improve the overall C budget toward a net storage, as reported by Ceschia et al. (2010) and Buysse et al. (2107). Moreover, our findings shown that the contribution of crop residue roughly corresponded

750 to the carbon deficit in Europe. Therefore, crop residue could play a key-role in land-based mitigation of anthropogenic emissions, as also reported by Stella et al. (2019). This is in line with the "*4 per 1000*" initiative (Rumpel et al., 2019) promoting the maintenance of soil fertility as a key to achieve GHG mitigation strategies. In addition to the spatial diversity observed on the European agricultural area, the achievement of this goal depends on the complexity of rural, economic, and political structure of the territories (Amundson and Biardeau, 2018). Furthermore, local policies can be supported by simulation tools

755 as used in this study, bearing in mind that their effectiveness can be affected by the omission of large variances given by varied characteristics of small extents. Finally, irrigation management extended to all European cropping land is able to increase the stored C (NEP = -3 %), but increase the contribution of $F_{C-harvest}$, $F_{C-residues}$ and the non-CO_2 GHG (up to +4 %), leading to slightly higher C deficits.

5   Conclusions and perspectives

760 In this study we presented the combined spatial analysis of two specific models for crops and grassland, to quantify the effects of climate change on the European agricultural systems. Results clearly showed that the productions will be stable in the first half of the century, while a strong reduction will occur during the second half of the century, especially at low latitudes, and mainly due to a reduction in the length of growing cycle. Non-CO_2 greenhouse gas emissions were triggered by the rising temperatures, increasing significantly in the second part of the century. At the EU scale, both grasslands and croplands are

765 potential carbon sinks, although this potential is reduced by the negative effects of climate change on productivity. Biomass removal from the agricultural surfaces (yield and hay), combined with the animal intake and the removal of crop residues, transformed the production systems into a net source of carbon. In this framework, the introduction of carbon with fertilizers and dung was not able to counterbalance these removals of C. Crop residues management could be an efficient strategy to improve the overall carbon balance towards a C neutrality, or even towards a C storage. Our study highlights that storing

770 further carbon in areas characterised by high levels of SOC will be more challenging in the future. The extension of irrigation to all European croplands highlights a significant increase of water demand over the next few decades for most of the European croplands, whereas the benefit in terms of crop yield will not contribute substantially to fill the gap of carbon losses.

Our findings prove that productivity, GHG emissions and soil C stock changes have a heterogeneous trend over time and space. This underlines the need of targeted agricultural policies at territorial scale aimed to avoid the risk of significant

775 reductions of productivity and mitigate the negative effects of climate change, foremost expected in the second half of the century. Accordingly, this transformational adaptation has to deal with socio-economic and political dynamics, as well as land suitability (Fischer et al., 2005; Chaudhary et al., 2018, Martin-Lopez et al., 2019). This work provides a solid database on

cultivation and management of cropland and grassland at a detailed spatial level, which can be exploited in future work to test different management options, new or a combination of ago-ecosystem models, climate change projections, crop varieties or

780 floristic compositions, and the support for future actions.

Author contribution

Conceptualization, M.C., R.M., K.K., R.S.M.; Data Curation, M.C., R.M.; Formal Analysis, M.C., R.M.; Funding acquisition, R.M., K.K., R.S.M.; Investigation, M.C., R.M., K.K., R.S.M.; Methodology, M.C., R.M., K.K., R.S.M.; Project administration, M.C., R.M., K.K., R.S.M.; Software, M.C., R.M.; Validation, M.C., R.M., K.K., R.S.M.; Visualization, M.C.; Writing –

785 original draft preparation, M.C.; Writing – review & editing, M.C., R.M., K.K., R.S.M.

Data availability

The datasets generated during and/or analysed during the current study are available from the corresponding author on reasonable request.

Acknowledgements

790 Funding for this study was provided by the European Union Seventh Framework Programme FP7/2007–2013 project Animal Change FP7-KBBE-2010 Project n° 266018, FACCE ERA-GAS project ResidueGAS and ADEME project AEGES. We would like to thank B. Gabrielle and J-L. Drouet who provided valuable support to this work.

References

Aguilera, E., Lassaletta, L., Sanz Cobeña, A., Garnier, J. & Vallejo Garcia, A. The potential of organic fertilizers and water
795   management to reduce N_2O emissions in Mediterranean climate cropping systems. Agric. Ecosyst. Environ. 164, 32–52 (2013).

Ammann, C., Neftel, A., Jocher, M., Fuhrer, J., and Leifeld, J. (2020). Effect of management and weather variations on the greenhouse gas budget of two grasslands during a 10-year experiment. Agric. Ecosyst. Environ. 292:106814. doi: 10.1016/j.agee.2019.106814

800 Amundson R., Biardeau L., 2018. Opinion: Soil carbon sequestration is an elusive climate mitigation tool. Proceedings of the National Academy of Sciences. 115. 11652-11656. 10.1073/pnas.1815901115.

Asseng, S., Ewert, F., Martre, P. et al. Rising temperatures reduce global wheat production. Nature Clim Change 5, 143–147 (2015). https://doi.org/10.1038/nclimate2470

Bahn M., Rodeghiero M., Anderson-Dunn M., Dore S., Gimeno C., Drösler M., Williams M., Ammann C., Berninger F.,
805   Flechard C., et al. Soil Respiration in European Grasslands in Relation to Climate and Assimilate Supply. Ecosystems 2008, 11, 1352–1367.

Bassu S., Brisson N., Durand J.-L., Boote K., Lizaso J., Jones J.W., Rosenzweig C., Ruane A.C., Adam M., Baron C., Basso B., Biernath C., Boogaard H., Conijn S., Corbeels M., Deryng D., De Sanctis G., Gayler S., Grassini P., Hatfield J.L., Hoek

S., Izaurralde C., Jongschaap R., Kemanian A.R., Kersebaum K.C., Kim S.-H., Kumar N.S., Makowski D., Müller C., Nendel C., Priesack E., Pravia M.V., Sau F., Shcherbak I., Tao F., Teixeira E., Timlin D., Waha K., 2014. How do various maize crop models vary in their responses to climate change factors? Glob. Change Biol., 20, no. 7, 2301-2320, doi:10.1111/gcb.12520.

Bouwman, Lex, Daniel, John S., Davidson, Eric A., de Klein, Cecile, Holland, Elisabeth, Ju, Xiaotang, Kanter, David, Oenema, Oene, Ravishankara, A.R., Skiba, Ute M., van der Sluis, Sietske, Sutton, Mark A., van der Werf, Guido R., Wallington, Timothy J., Wiesen, Peter, Winiwarter, Wilfried. 2013 Drawing down N2O to protect climate and the ozone layer. A UNEP Synthesis Report. United Nations Environment Programme (UNEP), 57pp.

Brilli, L., Bechini, L., Bindi, M., Carozzi, M., Cavalli, D., Conant, R., Dorich, C.D., Doro, L., Ehrhardt, F., Farina, R., Ferrise, R., Fitton, N., Francaviglia, R., Grace, P., Iocola, I., Klumpp, K., Léonard, J., Martin, R., Massad, R.S., Recous, S., Seddaiu, G., Sharp, J., Smith, P., Smith, W.N., Soussana, J.-F., Bellocchi, G., 2017. Review and analysis of strengths and weaknesses of agro-ecosystem models for simulating C and N fluxes. Sci. Total Environ. 598, 445–470.

Britz, W., Witzke, H., 2008. CAPRI Model Documentation 2008: Version 2 p, Institute for Food and Resource Economics, University of Bonn, Germany. available at: http://www.capri-model.org/docs/capri_documentation.pdf

Buysse P., Bodson B., Debacq A., De Ligne A., Heinesch B., Manise T., Moureaux C., Aubinet M. 2017. Carbon budget measurement over 12 years at a crop production site in the silty-loam region in Belgium, Agric. Forest Meteorol., 246, 241–255.

Calanca, P., Vuichard, N., Campbell, C., Viovy, N., Cozic, A., Fuhrer, J., Soussana, J.F., 2007. Simulating the fluxes of CO2 and N2O in European grasslands with the Pasture Simulation Model (PaSim). Agric. Ecosyst. Environ. 121, 164-174.

Cayuela, M.L., Aguilera, E., Sanz-Cobena, A., Adams, D.C., Abalos, D., Barton, L., Ryals, R., Silver, W.L., Alfaro, M.A., Pappa, V.A., Smith, P., Garnier, J., Billen, G., Bouwman, L., Bondeau, A., Lassaletta, L., 2017. Direct nitrous oxide emissions in Mediterranean climate cropping systems: emission factors based on a meta-analysis of available measurement data. Agric. Ecosyst. Environ. 238:25–35. https://doi.org/10.1016/j.agee.2016.10.006

Ceschia E., Beziat P., Dejoux J. F., Aubinet M., 2010. Management effects on net ecosystem carbon and GHG budgets at European crop sites, Agriculture, 139, 363–383

Chabbi, A., Lehmann, J., Ciais, P., Loescher, H. W., Cotrufo, M. F., Don, A., SanClements, M., Schipper, L., Six, J., Smith, P., Rumpel, C. (2017). Aligning agriculture and climate policy. Nature Climate Change, 7 (5), 307-309. , DOI : 10.1038/nclimate3286

Challinor, A.J., Watson, J., Lobell, D.B., Howden, S.M., Smith, D.R., Chhetri, N., 2014. A meta-analysis of crop yield under climate change and adaptation. Nat. Clim. Chang. 4, 287. https://doi.org/10.1038/nclimate2153.

Chang J., Ciais P., Viovy N., Soussana J.-F., Klumpp K., Sultan B., 2017. Future productivity and phenology changes in European grasslands for different warming levels: Implications for grassland management and carbon balance. Carbon Balance and Management, 12, 1–21. https://doi.org/10.1186/s13021-017-0079-8

Chang, J., Viovy, N., Vuichard, N., Ciais, P., Campioli, M., Klumpp, K., Martin, R., Leip, A., Soussana, J.-F. 2015. Modeled changes in potential grassland productivity and in grass-fed ruminant livestock density in Europe over 1961-2010. PLoS ONE, 10 (5), art. no. e0127554, DOI: 10.1371/journal.pone.0127554

Chaudhary, A., Gustafson, D., Mathys, A., 2018. Multi-indicator sustainability assessment of global food systems. Nat. Commun. 9, 848. https://doi.org/10.1038/s41467-018-03308-7.

Collins, W. J., Bellouin, N., Doutriaux-Boucher, M., Gedney, N., Halloran, P., Hinton, T., Hughes, J., Jones, C. D., Joshi, M., Liddicoat, S., Martin, G., O'Connor, F., Rae, J., Senior, C., Sitch, S., Totterdell, I., Wiltshire, A., and Woodward, S., 2011. Development and evaluation of an Earth-System model – HadGEM2, Geosci. Model Dev., 4, 1051–1075, https://doi.org/10.5194/gmd-4-1051-2011

Conant R.T., Cerri C.E.P., Osborne B.B., Paustian K., 2017. Grassland management impacts on soil carbon stocks: A new synthesis. Ecological Applications, 27 (2), pp. 662-668. DOI: 10.1002/eap.1473

Constantin, J., Raynal, H., Casellas, E., Hoffmann, H., Bindi, M., Doro, L., Eckersten, H., Gaiser, T., Grosz, B., Haas, E., Kersebaum, K.-C., Klatt, S., Kuhnert, M., Lewan, E., Maharjan, G.R., Moriondo, M., Nendel, C., Roggero, P.P., Specka,

855   X., Trombi, G., Villa, A., Wang, E., Weihermüller, L., Yeluripati, J., Zhao, Z., Ewert, F., Bergez, J.-E., 2019. Management
        and spatial resolution effects on yield and water balance at regional scale in crop models. Agricultural and Forest
        Meteorology, 275, pp. 184-195. DOI: 10.1016/j.agrformet.2019.05.013

        Cowan, N.J., Levy, P.E., Famulari, D., Anderson, M., Drewer, J., Carozzi, M., Reay, D.S., Skiba, U.M. 2016. The influence
        of tillage on N2O fluxes from an intensively managed grazed grassland in Scotland. Biogeosciences, 13 (16), pp. 4811-
860   4821. DOI: 10.5194/bg-13-4811-2016

        De Antoni Migliorati, M., Bell, M., Grace, P.R., Scheer, C., Rowlings, D.W., Liu, S. 2015. Legume pastures can reduce N2O
        emissions intensity in subtropical cereal cropping systems. Agriculture, Ecosystems and Environment, 204, pp. 27-39.
        10.1016/j.agee.2015.02.007

        de Souza, T.T., Silva Antolin S.L., Bianchini, V., Pereira, R., Moura Silva E., Marin F., 2019. Longer crop cycle lengths could
865   offset the negative effects of climate change on Brazilian maize. Bragantia. 78. 622-631. 10.1590/1678-4499.20190085.

        De Vries, W., Leip, A., Reinds, G. J., Kros, J., Lesschen, J. P., & Bouwman, A. F. (2011). Comparison of land nitrogen budgets
        for European agriculture by various modeling approaches. Environmental Pollution, 159(11), 3254–3268.
        doi:10.1016/j.envpol.2011.03.038

        Del Grosso SJ, Ojima DS, Parton WJ, Stehfest E, Heistemann M, DeAngelo B, et al. Global scale DAYCENT model analysis
870   of greenhouse gas emissions and mitigation strategies for cropped soils. Glob Planet Change. 2009; 67: 44±50

        Dono, G., Cortignani, R., Dell'Unto, D., Deligios, P., Doro, L., Lacetera, N., Mula, L., Pasqui, M., Quaresima, S., Vitali, A.,
        Roggero, P.P. (2016). Winners and losers from climate change in agriculture: insights from a case study in the
        Mediterranean basin. Agricultural Systems, 147, 65–75. https://doi.org/10.1016/j.agsy.2016.05.013.

        EEA – European Environment Agency (2020), Trends and projections in Europe 2020, Tracking progress towards Europe's
875   climate and energy targets: https://www.eea.europa.eu//publications/trends-and-projections-in-europe-2020

        Ehrhardt, F., Soussana, J.-F., Bellocchi, G., Grace, P., McAuliffe, R., Recous, S., Sándor, R., Smith, P., Snow, de Antoni
        Migliorati, Basso, B., Bhatia, A., Brilli, L., Doltra, J., Dorich, C. D., Doro, L., Fitton, N., Giacomini, S. J., Grant, B.,
        Harrison, M. T., Jones, S. K., Kirschbaum, M. U. F., Klumpp, K., Laville, P., Léonard, J., Liebig, M., Lieffering, Martin,
        R., Massad, R. S., Meier, E., Merbold, L., Moore, Myrgiotis, Newton, Pattey, Rolinski, S., Sharp, J., Smith, Wu, L., Zhang,
880   Q., 2018. Assessing uncertainties in crop and pasture ensemble model simulations of productivity and N2O emissions.
        Global Change Biology, 24 (2), e603-e616. , DOI : 10.1111/gcb.13965

        Emmel, C., Winkler, A., Hörtnagl, L., Revill, A., Ammann, C., D'Odorico, P., Buchmann, N., and Eugster, W.: Integrated
        management of a Swiss cropland is not sufficient to preserve its soil carbon pool in the long term, Biogeosciences, 15,
        5377–5393, https://doi.org/10.5194/bg-15-5377-2018, 2018.

885   European Commission, 2020. Communication from the commission to the European parliament, the council, the European
        economic and social committee and the committee of the regions Stepping up Europe's 2030 climate ambition Investing
        in   a   climate-neutral   future   for   the   benefit   of   our   people,   https://eur-lex.europa.eu/legal-
        content/EN/TXT/PDF/?uri=CELEX:52020DC0562&from=EN

        Eurostat,   2013.   Economy-wide   Material   Flow   Accounts   (EW-MFA)   -   Compilation   guide.
890   http://ec.europa.eu/eurostat/documents/1798247/6191533/2013-EW-MFA-Guide-10Sep2013.pdf/54087dfb-1fb0-40f2-
        b1e4-64ed22ae3f4c. Accessed on 07 September 2021.

        Eurostat, 2017. Agri-environmental indicator – greenhouse gas emissions. https://ec.europa.eu/eurostat/statistics-
        explained/index.php?title=Archive:Agri-environmental_indicator_-_greenhouse_gas_emissions&oldid=374989.
        Accessed on 07 September 2021.

895   Eurostat, 2019a. European Statistical Office database. Retrieved from: https://ec.europa.eu/eurostat/data/database

        Eurostat, 2019b. European Statistical Office database. Share of irrigable and irrigated areas in utilised agricultural area (UAA)
        by NUTS 2 regions. Retrieved from: http://appsso.eurostat.ec.europa.eu/nui/show.do?dataset=aei_ef_ir&lang=en

        Eurostat,   2020.   Annual   crop   statistics   handbook: 2020   edition   Retrieved   from:
        https://ec.europa.eu/eurostat/cache/metadata/Annexes/apro_cp_esms_an1.pdf

900 Ewert F., Van Ittersum M.K., Heckelei T., Therond O., Bezlepkina I., Andersen E., 2011. Scale changes and model linking methods for integrated assessment of agri-environmental systems. Agric. Ecosyst. Environ., 142, pp. 6-17. https://doi:10.1016/j.agee.2011.05.016

Fischer, G., Shah, M., Tubiello, F.N., von Velthuizen, H., 2005. Socio-economic and climate change impacts on agriculture: An integrated assessment, 1990-2080. Philosophical transactions of the Royal Society of London. Series B, Biological
905 sciences. 360. 2067-83. https://doi.org/10.1098/rstb.2005.1744.

Fitton, N., Alexander, P., Arnell, N., Bajzelj, B., Calvin, K., Doelman, J., Gerber, J. S., Havlik, P., Hasegawa, T., Herrero, M., Krisztin, T., van Meijl, H., Powell, T., Sands, R., Stehfest, E., West, P. C. and Smith, P. 2019. The vulnerabilities of agricultural land and food production to future water scarcity. Global Environmental Change, 58. 101944. ISSN 0959-3780. DOI: 10.1016/j.gloenvcha.2019.101944

910 Food and Agriculture Organization of the United Nations. FAOSTAT Database. Rome, Italy: FAO. Retrieved March 26, 2020 from http://www.fao.org/faostat/en/#home

Fuss, S., Jones, C.D., Kraxner, F., Peters, G.P., Smith, P., Tavoni, M., Van Vuuren, D.P., Canadell, J.G., Jackson, R.B., Milne, J., Moreira, J.R., Nakicenovic, N., Sharifi, A., Yamagata, Y., 2016. Research priorities for negative emissions. Environmental Research Letters, 11 (11) DOI: 10.1088/1748-9326/11/11/115007

915 Gabrielle, B., Da-Silveira, J., Houot, S., Michelin, J., 2005. Field-scale modelling of carbon and nitrogen dynamics in soils amended with urban waste composts. Agriculture. Ecosystems & Environment 110, 289e299. http://dx.doi.org/10.1016/j.agee.2005.04.015

Haas, E., Klatt, S., Fröhlich, A., Kraft, P., Werner, C., Kiese, R., Grote, R., Breuer, L., Butterbach-Bahl, K., 2013. LandscapeDNDC: A process model for simulation of biosphere-atmosphere-hydrosphere exchange processes at site and
920 regional scale. Landscape Ecology, 28 (4), pp. 615-636. DOI: 10.1007/s10980-012-9772-x

Hassink, J. and Whitmore, A. P., 1997. A Model of the Physical Protection of Organic Matter in Soils, Soil Sci. Soc. Am. J., 61, 131–139.

Hénault, C., Bizouard, F., Laville, P., Gabrielle, B., Nicoullaud, B., Germon, J.C., Cellier, P., 2005. Predicting in situ soil N2O emission using NOE algorithm and soil database. Global Change Biol. 11, 115-127.

925 Hiederer, R. 2013. Mapping Soil Properties for Europe - Spatial Representation of Soil Database Attributes. Luxembourg: Publications Office of the European Union - 2013 - 47pp. EUR26082EN Scientific and Technical Research series, ISSN 1831-9424, https://doi.org/10.2788/94128; Database: https://esdac.jrc.ec.europa.eu/content/european-soil-database-derived-data Accessed on 07 September 2021.

Hoffmann H., Zhao G., Asseng S., Bindi M., Biernath C., Constantin J., et al., 2016. Impact of Spatial Soil and Climate Input
930 Data Aggregation on Regional Yield Simulations. PLoS ONE 11(4): e0151782. doi:10.1371/journal.pone.0151782

Hörtnagl, L., Barthel, M., Buchmann, N., Eugster, W., Butterbach-Bahl, K., Díaz-Pinés, E., Zeeman, M., Klumpp, K., Kiese, R., Bahn, M., Hammerle, A., Lu, H., Ladreiter-Knauss, T., Burri, S., Merbold, L., 2018. Greenhouse gas fluxes over managed grasslands in Central Europe. Glob. Chang. Biol. https://doi.org/10.1111/gcb.14079

Howden SM, Soussana JF, Tubiello FN, Chhetri N, Dunlop M, Meinke H. 2007. Adapting agriculture to climate change. Proc.
935 Natl. Acad. Sci. USA 104:19691–96

Hsu J.S., Powell J., Adler P.B., 2012. Sensitivity of mean annual primary production to precipitation. Glob. Chang. Biol., 18, pp. 2246-2255.

IPCC, 2013. Climate Change 2013: The Physical Science Basis. Contribution of Working Group I to the Fifth Assessment Report of the Intergovernmental Panel on Climate Change. Stocker, T.F., Qin, D., Plattner, G.-K., Tignor, M., Allen, S.K.,
940 Boschung, J., Nauels, A., Xia, Y., Bex, V. and Midgley, P.M. Eds., Cambridge University Press, Cambridge, United Kingdom and New York, NY, USA, 1535. http://dx.doi.org/10.1017/CBO9781107415324

IPCC, 2018: Global warming of 1.5°C. An IPCC Special Report on the impacts of global warming of 1.5°C above pre-industrial levels and related global greenhouse gas emission pathways, in the context of strengthening the global response to the threat of climate change, sustainable development, and efforts to eradicate poverty [V. Masson-Delmotte, P. Zhai,

945   H. O. Pörtner, D. Roberts, J. Skea, P.R. Shukla, A. Pirani, W. Moufouma-Okia, C. Péan, R. Pidcock, S. Connors, J. B. R. Matthews, Y. Chen, X. Zhou, M. I. Gomis, E. Lonnoy, T. Maycock, M. Tignor, T. Waterfield (eds.)]

Jones, C. D., Hughes, J. K., Bellouin, N., Hardiman, S. C., Jones, G. S., Knight, J., Liddicoat, S., O'Connor, F. M., Andres, R. J., Bell, C., Boo, K.-O., Bozzo, A., Butchart, N., Cadule, P., Corbin, K. D., Doutriaux-Boucher, M., Friedlingstein, P., Gornall, J., Gray, L., Halloran, P. R., Hurtt, G., Ingram, W. J., Lamarque, J.-F., Law, R. M., Meinshausen, M., Osprey, S.,
950   Palin, E. J., Parsons Chini, L., Raddatz, T., Sanderson, M. G., Sellar, A. A., Schurer, A., Valdes, P., Wood, N., Woodward, S., Yoshioka, M., and Zerroukat, M., 2011. The HadGEM2-ES implementation of CMIP5 centennial simulations, Geosci. Model Dev., 4, 543–570, https://doi.org/10.5194/gmd-4-543-2011

Jones, C.A. and Kiniry, J.R., 1986. CERES-Maize: A simulation model of maize growth and development. Texas A&M University Press, Temple, TX, USA.

955   Jones, S. K., Helfter, C., Anderson, M., Coyle, M., Campbell, C., Famulari, D., Di Marco, C., van Dijk, N., Tang, Y. S., Topp, C. F. E., Kiese, R., Kindler, R., Siemens, J., Schrumpf, M., Kaiser, K., Nemitz, E., Levy, P. E., Rees, R. M., Sutton, M. A., Skiba, U. M., 2016. The nitrogen, carbon and greenhouse gas budget of a grazed, cut and fertilised temperate grassland, Biogeosciences, 14, 2069–2088, https://doi.org/10.5194/bg-14-2069-2017.

Kanter, D., Zhang, X., Mauzerall, D., Malyshev, S., Shevliakova, E., 2016. The importance of climate change and nitrogen
960   use efficiency for future nitrous oxide emissions from agriculture. Environmental Research Letters. 11. 094003. 10.1088/1748-9326/11/9/094003.

Kirschbaum, M.U.F., 1995. The temperature dependence of soil organic matter decomposition, and the effect of global warming on soil organic C storage. Soil Biology and Biochemistry, 27(6), 753–760. doi:10.1016/0038-0717(94)00242-s

Kutsch, W. L., Aubinet, M., Buchmann, N., Smith, P., Osborne, B., Eugster, W., Wattenbach, M., Schrumpf, M., Schulze, E.
965   D., Tomelleri, E., Ceschia, E., Bernhofer, C., Beziat, P., Carrara, A., Di Tommasi, P., Grünwald, T., Jones, M., Magliulo, V., Marloie, O., Moureaux, C., Olioso, A., Sanz, M. J., Saunders, M., Søgaard, H., and Ziegler, W., , 2010. The net biome production of full crop rotations in Europe, Agric. Ecosyst. Environ., 139, 336–345.

Lassaletta, L., Billen, G., Grizzetti, B., Anglade J., Garnier J., 2014. 50 year trends in nitrogen use efficiency of world cropping systems: The relationship between yield and nitrogen input to cropland. Environmental Research Letters. 105011. 105011.
970   10.1088/1748-9326/9/10/105011.

Lehmann, N., Finger R., Klein T., Calanca P, Walter A., 2013. Adapting crop management practices to climate change: Modeling optimal solutions at the field scale. Agric. Syst. 117: 55– 65.https://doi.org/10.1016/j.agsy.2012.12.011

Leip A, Britz W, Weiss F, de Vries, W., 2011. Farm, land, and soil nitrogen budgets for agriculture in Europe calculated with CAPRI. Environ Pollut 159:3243–3253. https://doi.org/10.1016/j.envpol.2011.01.040

975   Leip A, Marchi G, Koeble R, Kempen M, Britz W, Li C, 2008. Linking an economic model for European agriculture with a mechanistic model to estimate nitrogen and carbon losses from arable soils in Europe, Biogeosciences 5: 73–94, doi: 10.5194/bg-5-73-2008

Lesschen, J.P., van den Berg, M., Westhoek, H.J., Witzke, H.P., Oenema, O. 2011. Greenhouse gas emission profiles of European livestock sectors. Animal Feed Science and Technology, 166-167, pp. 16-28. DOI:
980   10.1016/j.anifeedsci.2011.04.058

Li X., Sørensen P., Olesen J. E., Petersen S. O., 2016. Evidence for denitrification as main source of N2O emission from residue-amended soil. Soil Biol. Biochem. 92, 153–160. doi: 10.1016/j.soilbio.2015.10.008

Lobell, D. B. and Tebaldi, C. 2014. Getting caught with our plants down: The risks of a global crop yield slowdown from climate trends in the next two decades, Environmental Research Letters. IOP Publishing, 9(7). doi: 10.1088/1748-
985   9326/9/7/074003.

Lugato E., Paniagua L., Jones A., de Vries W., Leip A., 2017. Complementing the topsoil information of the Land Use/Land Cover Area Frame Survey (LUCAS) with modelled N2O emissions. PLoS ONE 12(4): e0176111. DOI: 10.1371/journal.pone.0176111

Lugato, E., Bampa, F., Panagos, P., Montanarella, L., Jones, A., 2014. Potential carbon sequestration of European arable soils
990   estimated by modelling a comprehensive set of management practices. Global Change Biology, 20 (11), pp. 3557-3567.
DOI: 10.1111/gcb.12551

Lugato, E., Leip, A., Jones, A., 2018. Mitigation potential of soil carbon management overestimated by neglecting N2O
emissions. Nat. Clim. Chang. 8, 219–223.

Ma, S., Lardy, R., Graux, A.-I., Ben Touhami, H., Klumpp, K., Martin, R., & Bellocchi, G., 2015. Regional-scale analysis of
995   carbon and water cycles on managed grassland systems. Environmental Modelling & Software, 72, 356–371.
https://doi.org/10.1016/j.envsoft.2015.03.007

Maaz, T. M., Sapkota, T. B., Eagle, A. J., Kantar, M. B., Bruulsema, T. W., and Majumdar, K., 2021. Meta-analysis of yield
and nitrous oxide outcomes for nitrogen management in agriculture, Global Change Biology, vol. 27, no. 11, pp. 2343–
2360, 2021. https://doi:10.1111/gcb.15588

1000 Martínez-López J., Bagstad K.J., Balbi S., Magrach A., Voigt B., Athanasiadis I., Pascual M., Willcock S., Villa F., 2019.
Towards globally customizable ecosystem service models. Sci. Total Environ., 650, pp. 2325-2336,
10.1016/j.scitotenv.2018.09.371

Metzger, M. J., Bunce, R. G. H., Jongman, R. H. G., Mücher, C. A., & Watkins, J. W., 2005. A climatic stratification of the
environment of Europe. Global Ecology and Biogeography, 14(6), 549–563. https://doi.org/10.1111/j.1466-
1005 822X.2005.00190.x

Minasny, B., Malone, B.P., McBratney, A.B., Angers, D.A., Arrouays, D., Chambers, A., Chaplot, V., Chen, Z.-S., Cheng,
K., Das, B.S., Field, D.J., Gimona, A., Hedley, C.B., Hong, S.Y., Mandal, B., Marchant, B.P., Martin, M., McConkey,
B.G., Mulder, V.L., O'Rourke, S., Richer-de-Forges, A.C., Odeh, I., Padarian, J., Paustian, K., Pan, G., Poggio, L., Savin,
I., Stolbovoy, V., Stockmann, U., Sulaeman, Y., Tsui, C.-C., Vågen, T.-G., van Wesemael, B., Winowiecki, L., 2017. Soil
1010 carbon 4 per mille. Geoderma 292, 59–86.

Minoli, S., Müller, C., Elliott, J., Ruane, A.C., Jägermeyr, J., Zabel, F., Dury, M., Folberth, C., François, L., Hank, T.B.,
Jacquemin, I., Liu, W., Olin, S., & Pugh, T.A. 2019. Global response patterns of major rainfed crops to adaptation by
maintaining current growing periods and irrigation. Earth's Future 7, no. 12 (2019): 1464–80.
https://doi.org/10.1029/2018EF001130

1015 Molina, J.A.E., Clapp, C.E., Shaffer, M.J., Chichester, F.W., Larson, W.E., 1983. NCSOIL, a model of nitrogen and carbon
transformations in soil: description, calibration, and behavior. Soil Science Society of America Journal 47, 85-91.
http://dx.doi.org/10.2136/sssaj1983.03615995004700010017x

Morais T.G., Teixeira R.F., Domingos T., 2019. Detailed global modelling of soil organic carbon in cropland, grassland and
forest soils. PLoS ONE 14(9): e0222604. https://doi.org/10.1371/journal.pone.0222604

1020 Myrgiotis, V., Williams, M., Rees, R. M., and Topp, C. F. E.: Estimating the soil N2O emission intensity of croplands in
northwest Europe, Biogeosciences, 16, 1641–1655, https://doi.org/10.5194/bg-16-1641-2019, 2019.

Nicolardot, B., Molina, J.A.E., Allard, M.R., 1994. C and N fluxes between pools of soil organic matter: model calibration
with long-term incubation data. Soil Biology and Biochemistry 26, 235-243. http://dx.doi.org/10.1016/0038-
0717(94)90163-5

1025 Olesen J.E., 2017. Climate change impacts on society: Section 5.3: Agriculture. In Climate change, impacts and vulnerability
in Europe 2016: An indicator-based report. European Environment Agency 1/2017. pp. 223-244.

Olesen J.E., Bindi M., 2002. Consequences of climate change for European agricultural productivity, land use and policy. Eur.
J. Agron. 16, 239–262. https://doi.org/10.1016/S1161-0301(02)00004-7

Olesen J.E., Børgesen C.D., Elsgaard L., Palosuo T., Rötter R.P., Skjelvåg A.O., Peltonen-Sainio P., Börjesson T., Trnka M.,
1030 Ewert F., Siebert S., Brisson N., Eitzinger J., van Asselt E.D., Oberforster M., van der Fels-Klerx H.J., 2012. Changes in
time of sowing, flowering and maturity of cereals in Europe under climate change, Food Additives & Contaminants: Part
A, 29:10, 1527-1542, DOI: 10.1080/19440049.2012.712060

Olesen J.E., Trnka M., Kersebaum K.C., Skjelvåg A.O., Seguin B., Peltonen-Sainio P., Rossi F., Kozyra J., Micale F., 2011. Impacts and adaptation of European crop production systems to climate change. European Journal of Agronomy 34 (2):96-112.

Parry, M., Rosenzweig C., Livermore M., 2005: Climate change, global food supply and risk of hunger. Phil. Trans. Roy. Soc. B, 360, 2125-2138, doi:10.1098/rstb.2005.1751.

Parton, W.J., D.S. Schimel, D.S. Ojima, and C.V. Cole. 1994. A general model for soil organic matter dynamics: sensitivity to litter chemistry, texture and management. Pages 147-167 in R.B. Bryant and R.W. Arnold, editors. Quantitative modeling of soil farming processes. SSSA Special Publication 39. ASA, CSSA, and SSA, Madison, Wisconsin, USA.

Reinds GJ, Heuvelink GBM, Hoogland T, Kros J, De Vries W., 2012. Estimating nitrogen fluxes at the European scale by upscaling INTEGRATOR model outputs from selected sites. Biogeosciences. 9: 4527±4536.

Reuter, H.I, Rodriguez Lado, L., Hengl, T., Montanarella, L., 2008. Continental Scale Digital Soil Mapping using European Soil Profile Data: soil pH. - in Eds: Böhner,J. ,Blaschke,T. and Montanarella,L. SAGA – Seconds Out,; Hamburger Beiträge zur Physischen Geographie und Landschaftsökologie, Heft 19, Universität Hamburg, Institut für Geographie, ISSN: 1866-170X.

Riedo, M., Grub, A., Rosset, M., Fuhrer, J., 1998. A Pasture Simulation model for dry matter production, and fluxes of carbon, nitrogen, water and energy. Ecol. Model. 105, 141–183.

Rosenzweig C., Jones J. W., Hatfield J. L., Ruane A. C., Boote K. J., Thorburn P., Antle J. M., Nelson G. C., Porter C., Janssen S., Asseng S., Basso B., Ewert F., Wallach D., Baigorria G., Winter J. M., 2013. The Agricultural Model Intercomparison and Improvement Project (AgMIP): Protocols and pilot studies. Agric. For. Meteorol., vol. 170, pp. 166–172

Rumpel, C., Amiraslani, F., Chenu, C., Garcia Cardenas, M., Kaonga, M., Koutika, L.S., Ladha, J., Madari, B., Shirato, Y., Smith, P., Soudi, B., Soussana, J-F., Whitehead, D., Wollenberg, E., 2019. The 4p1000 initiative: Opportunities, limitations and challenges for implementing soil organic carbon sequestration as a sustainable development strategy. Ambio.: 1-11. https://doi.org/10.1007/s13280-019-01165-2

Sacks WJ, Deryng D, Foley JA, Ramankutty N., 2010.Crop planting dates: An analysis of global patterns. Glob Ecol Biogeogr. 19: 607-620.

Sándor R., Ehrhardt F., Brilli L., Carozzi M., Recous S., Smith P., Snow V., Soussana J.-F., Dorich C.D., Fuchs K., Fitton N., Gongadze K., Klumpp K., Liebig M., Martin R., Merbold L., Newton P.C.D., Rees R.M., Rolinski S., Bellocchi G., 2018. The use of biogeochemical models to evaluate mitigation of greenhouse gas emissions from managed grasslands, Science of The Total Environment, Volume 642: 292-306. http://dx.doi.org/10.1016/j.scitotenv.2018.06.020.

Schmid, M., Neftel, A., Riedo, M., and Fuhrer, J., 2001. Process-based modelling of nitrous oxide emissions from different nitrogen sources in mown grassland. Nutrient Cycling in Agroecosystems, 60(1):177–187.

Shcherbak I., Millar N., Robertson G.P., 2014. Global metaanalysis of the nonlinear response of soil nitrous oxide (N2O) emissions to fertilizer nitrogen. Proc. Natl. Acad. Sci. USA 111, 9199–9204.

Smit H.J., Metzger M.J., Ewert F., 2008. Spatial distribution of grassland productivity and land use in Europe. Agricultural Systems, 98 (3), pp. 208-219. DOI: 10.1016/j.agsy.2008.07.004

Smith P., 2016. Soil carbon sequestration and biochar as negative emission technologies. Global Change Biology 22, 1315–1324, doi: 10.1111/gcb.13178.

Smith P., 2012. Agricultural greenhouse gas mitigation potential globally, in Europe and in the UK: what have we learnt in the last 20 years? Global Change Biology, 18, 35–43.

Smith, P, Heberl, H, Popp, A, Erb, K-H, Lauk, C, Harper, R, Tubiello, F, De Pinto, A, Jafari, M, Sohi, S, Masera, O, Bottcher, H, Berndes, G, Bustamante, M, Ahammad, H, Clark, H, Dong, H, Elsiddig, E, Mbow, C, Ravindranath, N, Rice, C, Abad, C, Romanovskaya, A, Sperling, F, Herrero, M, House, J & Rose, S 2013, 'How much land based greenhouse gas mitigation can be achieved without compromising food security and environmental goals?', Global Change Biology, vol. 19, no. 8, pp. 2285-2302. https://doi.org/10.1111/gcb.12160

Smith, P., Martino, D., Cai, Z., Gwary, D., Janzen, H.H., Kumar, P., McCarl, B., Ogle, S., O'Mara, F., Rice, C., Scholes, R.J., Sirotenko, O., Howden, M., McAllister, T., Pan, G., Romanenkov, V., Schneider, U., Towprayoon, S., Wattenbach, M.,

Smith, J.U., 2008. Greenhouse gas mitigation in agriculture. Philosophical Transactions of the Royal Society B 27, 89–813.

Soussana J-F., Tallec T., Blanfort V., 2010. Mitigating the greenhouse gas balance of ruminant production systems through carbon sequestration in grasslands. Animal, 4, 334–350.

Soussana, J.F., Allard, V., Pilegaard, K., Ambus, C., Campbell, C., Ceschia, E., Clifton-Brown, J., Czobel, S., Domingues, R., Flechard, C., Fuhrer, J., Hensen, A., Horvath, L., Jones, M., Kasper, G., Martin, C., Nagy, Z., Neftel, A., Raschi, A., Baronti, S., Rees, R.M., Skiba, U., Stefani, P., Manca, G., Sutton, M., Tuba, Z. & Valentini, R. 2007. Full accounting of the greenhouse gas (CO2, N2O, CH4) budget of nine European grassland sites Agri, Eco. Enviro.,121: 121–134. DOI: 10.1016/j.agee.2006.12.022

Stagge, J.H., Kingston, D.G., Tallaksen, L.M., Hannah, D.M. Observed drought indices show increasing divergence across Europe. Sci. Rep. 2017, 7, 14045

Steduto, P., Hsiao, T.C., Fereres, E. and Raes, D., 2012. Crop Yield Response to Water. Irrigation and Drainage Paper 66, United Nations FAO, Rome.

Stehfest, E., Bouwman, L., 2006. N2O and NO emission from agricultural fields and soils under natural vegetation: summarizing available measurement data and modeling of global annual emissions. Nutrient Cycling in Agroecosystems 74: 207–228.

Stella T., Mouratiadou I., Gaiser T., Berg-Mohnicke M., Wallor E., Ewert F., Nendel, C., 2019. Estimating the contribution of crop residues to soil organic carbon conservation. Environmental Research Letters. Retrieved from http://iopscience.iop.org/10.1088/1748-9326/ab395c

Sutton M. & Billen G. Bleeker A., Erisman J.W., Grennfelt P., Grinsven H., Grizzetti B., Howard C., Leip A. 2011. European nitrogen assessment - Technical summary. European Nitrogen Assessment. XXXV-LI.

Tao F., Zhang Z., 2011. Impacts of climate change as a function of global mean temperature: maize productivity and water use in China. Climatic Change, 105, 409–432.

Tian, H., Xu, R., Canadell, J.G. et al. A comprehensive quantification of global nitrous oxide sources and sinks. Nature 586, 248–256 (2020). https://doi.org/10.1038/s41586-020-2780-0

Tubiello, F. N., Soussana, J. F., Howden, M. & Easterling, W., 2007. Crop and pasture responses to climate change: fundamental processes. Proceedings of the National Academy of Sciences 104, 19686–19690.

Tubiello, F.N & Rosenzweig, C. 2008. Developing climate change impact metrics for agriculture. The Integrated Assessment Journal, 8: 165–184.

Turral, H., et al. (2011), Climate change, water and food security, Water Rep., 36, Food and Agric. Organ., Rome.

USDA, 1994. Major World Crop Areas and Climatic Profiles. World Agricultural Outlook Board, U.S. Department of Agriculture. Agricultural Handbook No. 664.

Voglmeier, K., Six, J., Jocher, M., Ammann, C. 2019. Grazing-related nitrous oxide emissions: From patch scale to field scale. Biogeosciences, 16 (8), pp. 1685-1703. DOI: 10.5194/bg-16-1685-2019

Vuichard N, Ciais P, Viovy N, Calanca P, Soussana J-F (2007) Estimating the greenhouse gas fluxes of European grasslands with a process-based model: 2. Simulations at the continental level. Global Biogeochemical Cycles, 21, doi:10.1029/2005GB002612.

Wada Y., Wisser D., Eisner S., Flörke M., Gerten D., Haddeland I., Hanasaki N., Masaki Y., Portmann F.T., Stacke T., Tessler Z., Schewe J., 2013. Multimodel projections and uncertainties of irrigation water demand under climate change, Geophys. Res. Lett., 40, 4626–4632, https://doi.org/10.1002/grl.50686

Warszawski, L., Frieler, K., Huber, V., Piontek, F., Serdeczny, O., and Schewe, J., 2014. The Inter-Sectoral Impact Model Intercomparison Project (ISI-MIP): project framework, P. Natl. Acad. Sci. USA, 111, 3228–3232, https://doi.org/10.1073/pnas.1312330110

Wattenbach, M., Lüdtke, S., Redweik, R., Van Oijen, M., Balkovic, J., Reinds, G., 2015. A generic probability based model to derive regional patterns of crops in time and space. Geophysical Research Abstracts, Vol. 17, EGU2015-13153, 2015.

Weitz, A.M., Linder, E., Frolking, S., Crill, P.M., and Keller, M.. 2001. N2O emissions from humid tropical agricultural soils: Effects of soil moisture, texture and nitrogen availability. Soil Biol. Biochem. 33: 1077– 1093. doi: https://doi.org/10.1016/S0038-0717(01)00013-X

Wells, K. C., Millet, D. B., Bousserez, N., Henze, D. K., Griffis, T. J., Chaliyakunnel, S., Dlugokencky, E. J., Saikawa, E., Xiang, G., Prinn, R. G., O'Doherty, S., Young, D., Weiss, R. F., Dutton, G. S., Elkins, J. W., Krummel, P. B., Langenfelds, R., and Steele, L. P.: Top-down constraints on global N2O emissions at optimal resolution: application of a new dimension reduction technique, Atmos. Chem. Phys., 18, 735–756, https://doi.org/10.5194/acp-18-735-2018, 2018.

Wilkinson J.M., Lee M.R.F., 2017. Use of human-edible animal feeds by ruminant livestock. Animal, 1–9. https://doi.org/10.1017/S175173111700218X

Wint, G.R.W., Robinson, T.P., 2007. Gridded livestock of the world 2007. Food and Agriculture Organization of the United Nations (FAO), Rome, Italy, 131 p.

World Bank. World Development Indicators: Trends in greenhouse gas emissions. http://wdi.worldbank.org/table/3.9 Accessed on 07 September 2021.

Yang C., Fraga H., van Ieperen W., Trindade H., Santos J.A., 2019 Effects of climate change and adaptation options on winter wheat yield under rainfed Mediterranean conditions in southern Portugal. Clim. Chang., 154 (1), pp. 159-178

Yang X., Chen F., Lin X., Liu Z., Zhang H., Zhao J., et al., 2015. Potential benefits of climate change for crop productivity in China. Agricultural and Forest Meteorology, 208, 76–84. https://doi.org/10.1016/j.agrformet.2015.04.024

Zhang, Q., Zhang, W., Li, T., Sun, W., Yu, Y., Wang, G., 2017. Projective analysis of staple food crop productivity in adaptation to future climate change in China. Int. J. Biometeorol. 61, 1445–1460. https://doi.org/10.1007/s00484-017-1322-4.

Zhao C., Liu B., Piao S.L., Wang X.H., Lobell D.B., Huang Y., Huang M.T., Yao Y.T., Bassu S., Ciais P., Durand J.L., Elliott J., Ewert F., Janssens I.A., Li T., Lin E., Liu Q., Martre P., Muller C., Peng S.S., Penuelas J., Ruane A.C., Wallach D., Wang T., Wu D.H., Liu Z., Zhu Y., Zhu Z.C., Asseng S., 2017. Temperature increase reduces global yields of major crops in four independent estimates. Proc. Natl. Acad. Sci., 114, no. 35, 9326-9331, doi:10.1073/pnas.1701762114